

Efficient Forestation in the Brazilian Amazon: Evidence from a Dynamic Model^{*}

Rafael Araujo[†] Francisco Costa[‡] Marcelo Sant'Anna[§]

February 5, 2022

Abstract

This paper estimates the Brazilian Amazon's carbon-efficient forestation – i.e. when farmers internalize the social cost of carbon. We propose a dynamic discrete choice model of land use and estimate it using a panel of land use and carbon stock of 5.7 billion pixels between 2008 and 2017. Business-as-usual implies an inefficient release of 44 gigatons of CO_2 in the long run resulting from deforestation of an area twice the size of France. We find that relatively small carbon taxes can mitigate a substantial part of inefficient deforestation. We show that targeted mitigation efforts on areas with the largest potential for emission reductions can be very effective. We also find that while taxing cattle production can abate emissions, taxing crops is virtually innocuous.

JEL: Q23, Q54, Q15, C35, L73

Keywords: Deforestation, Carbon Emission, Amazon, Dynamic Discrete Choice Model.

*We thank Mike Abito, Juliano Assunção, Arthur van Benthem, Torfinn Harding, Roozbeh Hosseini, Kelsey Jack, Felipe Jordan, Michael Kiley, Wolfram Schlenker, Paul Scott, Joseph Shapiro, Eduardo Souza-Rodrigues, and seminar participants at the NBER EEE Spring Meeting, ASSA-AEA Meeting, AERE Summer Conference, GoSee, Ridge EEE, Barcelona GSE Summer Forum, KDI Frontiers in Development, joint MIT-Columbia-Stanford-Cornell Energy & Environmental Economics seminar, Wharton, University of Georgia, Insper, and FGV EPGE. Financial support is gratefully acknowledged from Rede de Pesquisa Aplicada FGV and from Coordenação de Aperfeiçoamento de Pessoal de Nível Superior - Brasil (CAPES) - Grant #001.

[†]FGV EPGE and Climate Policy Initiative. E-mail: carlquist.rafael@gmail.com.

[‡]University of Delaware. E-mail: fcosta@udel.edu.

[§]FGV EPGE. E-mail: marcelo.santanna@fgv.br.

1 Introduction

Limiting global warming hinges on a drastic reduction of global greenhouse gas emissions over the next decades. Mitigation pathways consistent with keeping peak warming within 1.5° Celsius above pre-industrial levels call for a 45% reduction in anthropogenic carbon dioxide (CO_2) emissions by 2030 relative to 2010's levels (Rogelj et al., 2018). In fact, all but one mitigation pathways proposed by the last assessment of the Intergovernmental Panel on Climate Change (IPCC) counts on agriculture and land use reaching net-zero emissions by 2030, in particular, by reducing deforestation in tropical ecosystems.¹

Tropical forests hold an extraordinary amount of carbon in the form of biomass. Deforestation, especially using fire to clear the land, releases this carbon into the atmosphere. This makes forest clearing the main element responsible for CO_2 emissions in tropical ecosystems (IPCC, 2007). For instance, the Brazilian Amazon alone stored the equivalent of more than 200 gigatons of CO_2 in 2000, the equivalent to the last 35 years of the United States fossil fuels emissions. Since then, land-use changes in the Brazilian Amazon released 16.65 gigatons of CO_2 (De Azevedo et al., 2018). At this pace, by 2030 deforestation in the Brazilian Amazon will have released additional 6.7 gigatons of CO_2 . Forest conservation, therefore, is key to limiting global warming. Moreover, forests regulate micro-climate with implications for agriculture and water security (Spracklen et al., 2012), and tropical forests hold immeasurable biodiversity value.

While preserving tropical forests has great global social value, alternative uses of land can be profitable for the local population. The main driver of forest loss in the Brazilian Amazon has been the expansion of pasture for extensive cattle ranching. In our study period, between 2008 and 2017, 90% of the deforested area was converted to pasture. By 2017, pasture covered 13% of the Brazilian Amazon, and cropland only 2%. Although cattle ranching achieves low productivity in most of the region, high productivity cash crops, such as soy and maize, are also grown in the region. This indicates sizable spatial heterogeneity of the disposition of the private benefits from exploiting the land (e.g., returns from agriculture), and the social cost of deforestation (e.g., carbon storage).

Thus, the analysis of the implications for climate change of land use in tropical forests needs to take into account such spatial heterogeneity. Also, as we are fundamentally interested in how the dynamics of land use will shape the amount of carbon released from the forest over time, one needs to account for both the dynamic costly adjustments of land use and the social value of preserving the carbon stored in the land.

¹The only exception is the scenario in which carbon dioxide removal technologies will be available at a massive scale by 2050 (mitigation pathway S5 in Rogelj et al., 2018).

In this paper, we estimate the carbon-efficient forest cover and stock of carbon in the Brazilian Amazon in the long run. We assess how environmental policies based on geographical characteristics of the forest and market-based incentives can reduce the gap between the long-run stock of carbon under business-as-usual land use and carbon-efficient land use. To do so, we propose a dynamic discrete choice model where profit-maximizing farmers choose the land use taking into account conversion costs and flow returns from alternative land uses. In our model, the carbon-efficient land use is the one in which farmers fully internalize the social value of the carbon stored in the forest when choosing whether to preserve the vegetation or to convert it into pasture or cropland. We restrict attention to this precise definition of efficiency because we have access to state-of-the-art granular measurements of aboveground biomass stored in each plot of the entire forest. However, our framework is general and could include other externalities linked to deforestation.²

Our model enables us to use the flow of land-use choices to estimate its primitives and, therefore, compute the steady-state stock of carbon in the Brazilian Amazon under different scenarios.³ We follow steps similar to Scott (2018) to derive an Euler equation that serves as a regression in which land-use transition probabilities form the dependent variable. This model-based regression is the cornerstone of our estimation approach to recover the model structural parameters.⁴

We estimate the model with a rich panel dataset that classifies the land use of more than 5.7 billion pixels – at 30 meters resolution – for each year from 2008 to 2017 in the Brazilian Amazon (MapBiomass, 2019). We model the return of agriculture by combining potential yield for each crop (FAO GAEZ, 2012) with local prices data of agricultural products at the regional major trade hubs, and newly computed transportation cost.⁵ We model the private opportunity cost of the carbon stored in the land as a function of the amount of aboveground biomass stored in the vegetation of each pixel in 2000 (Zarin et al., 2016). We study the years between 2008 and 2017 when the region was under a relatively stable environmental regulatory framework. We focus on forested pixels outside protected areas (i.e. indigenous

²Quantifying the marginal effect of deforesting each plot of forest on the value of the biodiversity stored in the forest, or on micro-climate regularization, is extremely challenging and outside the scope of this paper.

³A dynamic model is warranted because when there are fixed land conversion costs, the responses to permanent changes in land use returns will be different than responses to typical transitory returns variation (e.g., prices) seen in the data. In fact, Scott (2018) shows that cropland elasticities based on static models fail to quantify all adjustments to changes in prices as compared with those based on dynamic models.

⁴This approach is generalized by Kalouptsidi et al. (2021) and also similar to Aguirregabiria and Magesan (2013). An advantage of this method is that it does not require assumptions on how agents make expectations about future prices and market conditions (c.f., Hendel and Nevo, 2006; Gowrisankaran and Rysman, 2012).

⁵We estimate transportation costs of each crop from any pixel in the region to international markets following Donaldson (2018). We build a complete transportation network of Brazil including roads, ports, and waterways. We then fit a non-linear least squares model of freight cost to monetize transportation costs.

land or conservation units) because protected areas are subject to specific regulations.

In our model, the amount of carbon in a plot of forest affects farmers' decisions through a private perceived carbon value, that captures two elements. First, a perceived carbon value imposed implicitly by Brazilian environmental laws and enforcement. Second, the private costs and benefits associated with the environmental services provided by forest density (e.g., preventing soil erosion). We estimate that the perceived carbon value that rationalizes observed land-use choices is \$7.26 per ton of CO_2 . This suggests that environmental regulation in the Brazilian Amazon helps farmers to partially internalize the social value of the forest. However, farmers' perceived value of carbon falls short of recent estimates of the social cost of carbon, centered around \$50 per ton (EPA, 2016).

We compute the efficient steady-state forest cover and stock of carbon as the one in which agents fully internalize the social cost of carbon of \$50 per ton of CO_2 . Our counterfactuals show the gap in steady-state emissions under the business-as-usual land use and the efficient land use is 44 gigatons of CO_2 . That is, on the long run, the equivalent to eight times United States' emissions of fossil fuels in 2018 (Friedlingstein et al., 2019) – or twice the CO_2 emissions from land-use change in Brazil in the last twenty years (De Azevedo et al., 2018) – would be *inefficiently* released from the forest under the business-as-usual land use. This would imply that the Brazilian Amazon would be short 1,075,000 km^2 of forest cover to its efficient forestation on the steady state – this is approximately two times the size of France.

We then quantify the effectiveness of two policy instruments to set land use closer to its efficient path. We first calculate how a tax that increases the perceived carbon value could shape farmers' incentive to deforest. We can interpret this policy as an implied-carbon tax (or subsidy) that changes the private forest return – e.g., increased enforcement or providing payment for ecosystem services. We find that farmers' response to a carbon tax is convex. A carbon tax of \$2.5 per ton of CO_2 stored in the forest would prevent 16 gigatons of CO_2 from being released in the steady state, implementing 34% of the socially efficient carbon emission reduction relative to business-as-usual land use. A carbon tax of \$10/ton would preserve 37 gigatons of CO_2 , mitigating 84% of the inefficient emissions in the steady state. Intuitively, land is the main input for the expansion of cattle ranching, so relatively small increases in the perceived cost of deforesting the marginal plot represent a substantial increase on the cost structure of ranchers.

We further exploit the spatial dimension of our model to quantify the effectiveness of targeted mitigation efforts. We show that targeting the carbon tax on the top quartile of pixels with the largest potential for emission reductions would preserve more than half of the emissions as compared to the same tax implemented in the whole region. While it may be

expensive to target some policies at the pixel level, we also use our model to inform targeting at more aggregate administrative levels.

Alternatively, we consider an excise tax on cattle ranching or crop production. Our counterfactuals show that a 20% tax on the returns of cattle ranching would induce the same reduction in emissions as a \$2.5/ton carbon tax, and a 65% tax would induce the same emissions reduction as a \$10/ton carbon tax. Taxing crops has virtually no effect on emissions, as this activity still occupies a small share of this region. This highlights the humongous public policy effort needed to mitigate carbon emissions in this context, as only very large excise taxes could substantially mitigate the efficient forestation gap.

A large literature studies optimal policies to fight deforestation (e.g., Pattanayak et al., 2010; Assunção et al., 2019b; Dominguez-Iino, 2021; Hsiao, 2021). From this literature, our paper is closest to Souza-Rodrigues (2019), which estimates the demand for deforestation in the Brazilian Amazon using a static discrete choice framework and municipality level data. Our main contribution is to compute carbon-efficient forestation in the long run and to investigate how policies can shape the carbon stored in the forest in the long run. To do this, we make two key innovations. First, land use is a sluggish process and static models can underestimate land use elasticities (Scott, 2018). Because we are interested in the long-run forestation, we propose a dynamic model.⁶ Second, we need to take into account that carbon density is not homogeneous in the whole region, so we use remote sensing data on the stock of biomass in each forested pixel. This allows us to compare the net private benefits and the social costs of deforestation at the pixel level.

A growing literature studies land-use decisions using static general equilibrium environments (e.g., Costinot et al., 2016; Donaldson and Hornbeck, 2016; Pellegrina, 2020). Nevertheless, to study general equilibrium effects in a tractable framework, these models abstract from forward-looking behavior and lumpy adjustments. A similar point can be made about the large literature that estimates the treatment effects of different policies used to mitigate deforestation (e.g. Alix-Garcia et al., 2015; Jayachandran et al., 2017) and about discrete choice approaches that capture dynamic incentives using a reduced form model (e.g., Lubowski et al., 2006; Heilmayr et al., 2020). The literature focused on the Brazilian Amazon has shown that, in fact, policies implemented during the 2000s were very effective in reducing deforestation by 70% in a very short period.⁷ Our results quantify the potential

⁶Hsiao (2021) also employs a dynamic empirical model to study how coordination on international climate action influences the expansion of palm oil plantations in Indonesia. In his setting, deforestation is irreversible which may lead to non-stationary long-run dynamics. As we observe substantial forest regeneration (Assunção et al., 2019a) (e.g., 13% of pasture areas in 2008 converted back to forests in 2017), deforestation in our model is not an irreversible process.

⁷E.g., Nepstad et al. (2014); Assunção et al. (2015); Assunção and Rocha (2019); Burgess et al. (2019).

long-run emission reductions of enhancing this set of policies in the region.

An important methodological contribution is that by using granular data on carbon stock, we disentangle the loss of forest cover from CO_2 emissions, and show that both variables are not linearly related as usually assumed. As noted in Assunção et al. (2019b), targeting environmental policies in a situation where the government budget is over-stretched can be of great importance. Here, we present a microfounded model that allows us to implement location-specific policies according to the potential of emission reduction. This can be especially relevant to mitigate the effect of policies that are known to put pressure on deforestation in designated areas, such as infrastructure building, the demarcation of protected areas, or zoning regulations.⁸

Finally, we also contribute to the literature discussing cropland responses to prices and the economic environment (Chomitz and Gray, 1999; Lubowski et al., 2006; Fezzi and Bateman, 2011; Scott, 2018; Sant'Anna, 2021). Our model estimates allow us to understand how farmers' land-use choices are affected by prices in the long run. We find a long-run cropland elasticity with respect to crop prices higher than Scott (2018) estimate for the United States, even though we find a strong substitution effect between pastureland and cropland. This highlights different land-use dynamics of a consolidated developed agricultural region – such as the United States – from a developing agricultural frontier – such as in low- and middle-income countries. Our results are consistent with the ones found by Sant'Anna (2021) when studying sugarcane expansion in Brazil, using different data and estimation methods.

The paper proceeds as follows. Section 2 presents an overview of land use and deforestation in the Brazilian Amazon. Section 3 presents our model and derives the regression used to recover the model's parameters. Section 4 describes the data used to estimate the model. Section 5 discusses the identification, estimation, and our estimates. We present the counterfactual results in Section 6. We discuss the main caveats of our exercise and present some extensions in Section 7, and we give our concluding remarks in Section 8.

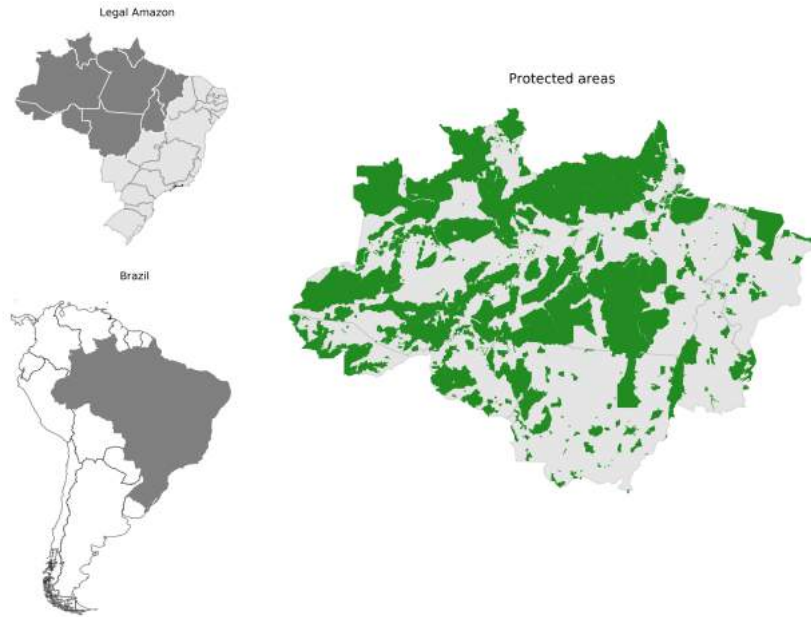
2 Background

We start with a brief background on the key elements of our empirical setting that guide our model. We study land use in the Legal Amazon territory in Brazil, the administrative region that includes the Amazon biome and that is subject to specific environmental and land use regulation. This region, depicted in Figure 1, covers more than five million squared

⁸E.g., Asher et al. (2020); Soares-Filho et al. (2010); Nolte et al. (2013); Alix-Garcia et al. (2018); Harding et al. (2021).

km (61% of Brazilian territory). In 2000, forest covered 84% of the Legal Amazon area. After years of peak deforestation, the Brazilian government implemented a series of new environmental regulations and strengthened enforcement capacity between 2004 and 2007. Among other policies, the government created new protected areas (indigenous land and conservation units) and toughened the penalties for environmental crimes. The conservation policies implemented in this period were very effective to reduce deforestation in the following decade (e.g., Assunção et al., 2015; Burgess et al., 2019). We thus study the period between 2008 and 2017 when the Legal Amazon region was under this new regulatory framework. We focus only on unprotected areas in our sample because land inside protected areas (the green area in the map on the right of Figure 1, which accounts for 55.9% of the Legal Amazon) are subject to specific regulation, for example, it is not allowed to grow cash crops.

Figure 1: Legal Amazon Excluding Protected Areas (in green)



The figure shows the Legal Amazon territory and the Brazilian states. Our sample consists of the Legal Amazon area excluding the protected areas marked in green.

The most important agricultural activity in the region is cattle ranching, accounting for 21% of the land use in our sample. Atomistic ranchers raise cattle in the region in extensive operations. Cattle then moves up the supply chain for finishing in a concentrated downstream meatpacking industry (Dominguez-Iino, 2021). About 80% of the beef produced in Brazil is consumed domestically. In our sample, crops accounted for only 3% of the land use in 2008, but they are steadily expanding in the region, accounting for 4% of the area in 2017. The two main crops produced are soybeans and maize, accounting for 73% of total cropland.

Soybeans and maize production in Brazil are mainly export-oriented, with producer prices determined in international markets.

Geographical determinants (e.g., soil, climate, trade costs, and other fixed land characteristics) are crucial to understanding land-use choices for agricultural production (Bustos et al., 2016; Costinot et al., 2016; Pellegrina, 2020). These factors will also be important in our context, especially transportation costs. Production in the Amazon relies on a sparse road network complemented by river waterways to reach destination markets (Souza-Rodrigues, 2019). Cattle and beef production relies on road networks and makes little use of waterways. In extensive areas of the Amazon rainforest, those transportation costs are prohibitive.

Table 1 summarizes land use and land transitions in our sample of unprotected areas. Each cell in columns (3) to (5) indicates the share of fields converting from land use ‘row’ in 2008 to land use ‘column’ in 2017. We can see that the main driver of forest cover loss in the region has been the expansion of pasture for cattle ranching. Only 0.8% of areas classified as forests in 2008 transitioned to crops in 2017, while an area nine times larger transitioned from forest to pasture. Forest clearing is typically done using fire, releasing the carbon stored in the vegetation with dire consequences that go beyond climate change. After clearing, preparing the land for agriculture involves sunk costs, such as removing stumps and leveling the terrain.

Forest regeneration. We also learn from transition rates that deforestation in our setting is not a one-way street. Forest regeneration is relatively common: 13% of pasture areas in 2008 converted back to forests in 2017. Forest regeneration in the region happened without active policies that promoted it, although regeneration may be a side effect of the stricter regulatory framework after 2004 (Assunção et al., 2019a).

The relatively high transition rates of agricultural activities to forests, although under-studied, constitute a relevant phenomenon that cannot be ignored when thinking about the dynamics of land use in the Amazon. We discuss forest regeneration next – see Appendix C for additional evidence.

First, we use additional data to document that regeneration is indeed sizeable. Between 45,000 to 70,000 squared km in our sample are secondary vegetation. Those are areas that are growing back forest after being previously deforested. This amounts to between 3% and 5% of the total forest area in any given year in our sample. This seems too large to be accounted for by measurement errors in the land classification process. In MapBiomas project cross-validation exercises, just 1.18% of forest areas were misclassified as agriculture.⁹

⁹We further discuss potential misclassification issues in Section 4.

Table 1: Land Use Shares and Transitions in the Legal Amazon

Land use share		Land use transitions from 2008 (row) to 2017 (column)		
		Forest	Crop	Pasture
(1)	(2)	(3)	(4)	(5)
Forest	0.72	0.920	0.008	0.065
Crop	0.03	0.030	0.890	0.074
Pasture	0.21	0.130	0.054	0.810

Columns (1) and (2) report land use shares for each category in 2008 and 2017, respectively. In columns (3) to (5), each cell indicates the share of fields transitioning from land use ‘row’ in 2008 to land use ‘column’ in 2017. Rows do not add up to one because we omit the ‘other’ category – i.e., non-classified pixels, urban areas, and water.

Second, we show that regeneration is more common in areas with degraded pastures, and thus less profitable for farming. That is, the own nature of cattle ranching in the region – that uses extensive grazing – leads farmers to cease agricultural operations in some fields. Over time, a natural regeneration process starts in these abandoned fields.

Other mechanisms could also be in place, which are outside the scope of our modeling framework, such as the action of land grabbers and illegal loggers. However, logging is typically associated with forest degradation rather than deforestation (Matricardi et al., 2020) and evidence suggests that illegal logging in the Amazon region receded by the end of the 2000’s (Chimeli and Soares, 2017). Unfortunately, the lack of precise data about these activities prevents a thorough examination of those mechanisms in our context.

3 Model

We formulate a dynamic discrete choice model where every year a profit-maximizing agent chooses how to use each plot of land. The agent can convert between different land uses subject to conversion costs. In this section, we derive the structural regression equation that serves as the basis of our estimation approach.

3.1 Setup

The basic unit of decision in the model is a field, denoted by i . Fields are grouped in locations, denoted by m .¹⁰ Each field i is run by a rational agent that chooses the profit-maximizing land use. These agents may formally own, lease or just hold informal property rights over the land. We only require they are residual claimants over the net discounted cash flow of their farming operation. Agents can choose among three possible land uses $j \in J = \{crop, pasture, forest\}$. That is, they can plant cash crops, use the land as pasture for cattle grazing or leave it unused, typically, covered by native vegetation. This choice is repeated every year $t = 1, 2, \dots, \infty$.

Each land use choice generates a profit flow $\pi_j(w_{mt}, \varepsilon_{imjt})$ in year t that depends on a vector of location specific state variables $w_{mt} \in \mathbb{R}^L$ – which include observable (*e.g.*, prices, land characteristics, transportation costs) and unobservable (to the econometrician) variables – and $\varepsilon_{imjt} \in \mathbb{R}$ which are field, choice and time specific shocks unobservable to the econometrician. We assume a separable structure for the profit function:

$$\pi_j(w_{mt}, \varepsilon_{imjt}) = r_j(w_{mt}; \alpha) + \varepsilon_{imjt}, \quad (1)$$

where $r_j(\cdot; \alpha)$ is a known function up to parameters α .

Agents must pay a land conversion cost $\Phi(j, k)$, where $j \in J$ denotes the current land use and $k \in J$ denotes the previous period land use. For instance, $\Phi(pasture, forest)$ denotes the cost (or benefit) from deforestation and conversion of the field to pasture.

Assumption 1 *The evolution of location-specific state variables follows a Markov process and it is conditionally independent from field level information (decisions and characteristics) – i.e., $F(w_{m,t+1}|w_{m,t}, \varepsilon_{imjt}, j) = F(w_{m,t+1}|w_{m,t})$.*

Assumption 1 implies that field-level decisions and characteristics do not affect the evolution of market-level variables. This is consistent with the idea that agents are price takers in competitive final product markets.

Assumption 2 *Field level shocks ε_{imjt} are independent over time and choices conditional on field characteristics and market-level state variables, with type-I extreme value distribution.*

Assumption 2 is standard in the dynamic discrete choice literature. Assumptions 1 and 2 allow us, under usual regularity conditions, to write the agent's dynamic land use choice

¹⁰In our application, a field corresponds to 30m resolution pixel from satellite imagery, while a location stands for a coarser 1km grid where individual fields are grouped.

problem with Bellman equations. The problem of an agent in period t , with land use k in period $t - 1$ is:

$$V(k, w_{mt}, \varepsilon_{imt}) = \max_{j \in J} \{ \Phi(j, k) + r_j(w_{mt}; \alpha) + \varepsilon_{imjt} + \rho E [\bar{V}(j, w_{m,t+1})|w_{mt}] \}, \quad (2)$$

where $\bar{V}(j, w_{mt}) = E_\varepsilon [V(j, w_{mt}, \varepsilon_{imt})]$, $\varepsilon_{imt} \in \mathbb{R}^3$ is the vector of shocks ε_{imjt} for each choice $j \in J$, and ρ is the discount rate. We denote the non-random component of equation (2) as

$$v(j, k, w_{mt}) = \Phi(j, k) + r_j(w_{mt}; \alpha) + \rho E [\bar{V}(j, w_{m,t+1})|w_{mt}]. \quad (3)$$

We can then re-write the agent's problem as

$$V(k, w_{mt}, \varepsilon_{imt}) = \max_{j \in J} \{ v(j, k, w_{mt}) + \varepsilon_{imjt} \}. \quad (4)$$

The distributional assumption on field level shocks (Assumption 2) implies the logit conditional choice probability:

$$p(j|k, w_{mt}) = \frac{\exp(v(j, k, w_{mt}))}{\sum_{j' \in J} \exp(v(j', k, w_{mt}))}, \text{ for } k, j \in J. \quad (5)$$

This is the probability a field transitions from land use k to land use j conditional on w_{mt} . The formulation above yields the Hotz and Miller (1993) inversion:

$$\log \left(\frac{p(j|k, w_{mt})}{p(j'|k, w_{mt})} \right) = v(j, k, w_{mt}) - v(j', k, w_{mt}), \text{ for } k, j, j' \in J. \quad (6)$$

That is, the ratio of conditional choice probabilities of different alternatives is directly related to the difference between the non-random components of returns from these alternatives.

Assumption 3 $\Phi(j, j) = 0$ for all $j \in J$ – i.e., there is no conversion cost if land is not converted.

From equations (3) and (6), using Assumption 3, we can write an expression reminiscent of an Euler equation:

$$\begin{aligned} \log \left(\frac{p(j|k, w_{mt})}{p(k|k, w_{mt})} \right) - \rho \log \left(\frac{p(j|k, w_{m,t+1})}{p(j|j, w_{m,t+1})} \right) &= (1 - \rho)\Phi(j, k) + \\ r_j(w_{mt}; \alpha) - r_k(w_{mt}; \alpha) + \eta_j^V(w_{mt}) - \eta_k^V(w_{mt}), \text{ for } j, k \in J, \end{aligned} \quad (7)$$

where $\eta_j^V(w_{mt}) = \rho(E [\bar{V}(j, w_{m,t+1})|w_{mt}] - \bar{V}(j, w_{m,t+1}))$ denotes the expectation error in

continuation values (see Appendix A for details). This derivation relies on the one-period finite dependence property that holds for our model: if j is picked in $t+1$, it does not matter for future choices ($t+2$ onwards) if either j or k were chosen in t . It allows us to eliminate continuation values and write an optimality condition based on choices in two consecutive periods, similar to a typical Euler equation (see Scott, 2018).¹¹

It will be useful now to separate the location specific state vector w_{mt} into its observable and unobservable components. That is, $w_{mt} = (x_{mt}, \xi_{mt})$, where $x_{mt} \in \mathbb{R}^{L-3}$ is a vector of observed variables and $\xi_{mt} \in \mathbb{R}^3$ is a vector of choice specific unobserved state variables. We require $r_j(\cdot; \alpha)$ to be linear in α with an additive location and choice specific unobservable:

$$r_j(w_{mt}; \alpha) = \bar{\alpha}_j + \alpha'_j R_j(x_{mt}) + \xi_{jmt}, \text{ for } j \in J, \quad (8)$$

where $R_j(x_{mt})$ is a choice specific known function of observables, and $\bar{\alpha}_j$ is an intercept. The specific formulation for $R_j(\cdot)$ will be shaped by data availability and discussed in detail in the next subsection.

Structural regression equation. Finally, we recover a regression equation by substituting (8) into (7):

$$\log \left(\frac{p(j|k, w_{mt})}{p(k|k, w_{mt})} \right) - \rho \log \left(\frac{p(j|k, w_{m,t+1})}{p(j|j, w_{m,t+1})} \right) = (1 - \rho)\Phi(j, k) + \alpha'_j R_j(x_{mt}) - \alpha'_k R_k(x_{mt}) + \bar{\alpha}_j - \bar{\alpha}_k + \xi_{jmt} - \xi_{kmt} + \eta_j^V(w_{mt}) - \eta_k^V(w_{mt}), \text{ for } j, k \in J. \quad (9)$$

The left-hand side depends only on conditional choice probabilities that can be observed (estimated) directly from the data. On the right hand side, we have regressors $R_j(x_{mt})$ and $R_k(x_{mt})$, aggregate shocks ξ_{jmt} and ξ_{kmt} , and an structural error $\eta_j^V(w_{mt}) - \eta_k^V(w_{mt})$. Given our assumption that agents hold rational expectations, the structural error is the difference between expected and realized continuation value. These are true error terms with mean zero conditional on information at t and transition specific intercept terms.

We let the $\bar{\alpha}_j$ absorb choice-specific components which are constant across locations and time. This implies ξ_{jmt} is mean zero across locations and time. Because ξ_{jmt} and $\bar{\alpha}_j$ always appear as a sum, this a true normalization and innocuous to any counterfactual we consider.

To disentangle conversion costs $\Phi(j, k)$ from $\bar{\alpha}_j$ and $\bar{\alpha}_k$, we need to assume a grounding condition. We assume that forest regeneration in our data set is driven by land left idle.

¹¹ Aguirregabiria and Magesan (2013) formalizes the connection between the continuous choice Euler equation and the dynamic discrete choice setting using the powerful abstraction that agents choose conditional choice probabilities (which are continuous) ahead of idiosyncratic shock realizations.

Therefore there are no costs when transitioning from pasture or crop back to forest. This is a natural assumption in our setting because the extent of active reforestation in the Amazon is minimal.

Assumption 4 *The fixed conversion cost from crop or pasture to forest is zero – i.e., $\Phi(\text{forest}, \cdot) = 0$.*

3.2 Flow of profits

We now discuss our specification of flow profits $r_j(\cdot; \alpha)$ in equation (1) for each choice of land use. These specifications are mainly context and data-driven. Our presentation here will anticipate many of the covariates we have gathered for our analysis. We further discuss the data in Section 4.

Crop. In our setting, agriculture gives us a natural structure of flow profits for the crop land use. All products produced in each parcel of land could be transported to destination markets and sold at market price. The net revenue from this operation is equal to

$$(p_{ct} - z_{mc})y_{mc} + \bar{\alpha}_{crop} + \xi_{crop,m,t}, \quad (10)$$

where y_{mc} is the expected yield of crop c in location m , p_{ct} is the output price in destination markets, z_{mc} is the transportation cost from location m to destination markets, and $\bar{\alpha}_{crop} + \xi_{crop,m,t}$ is a fixed cost associated with the crop land use that absorbs costs with inputs, wages, and other unobserved factors that are allowed to vary across locations and time.

We do not observe which crop is produced in each parcel. Instead, we use a weighted average of crops produced in location m 's region:

$$\tilde{r}_{mt} = \sum_{c \in \mathcal{C}} s_{cm} (p_{ct} - z_{mc}) y_{mc}, \quad (11)$$

where s_{cm} is the share of crop c in location m 's region. Thus the net payoff for crop becomes:

$$r_{crop}(w_{mt}; \alpha) = \alpha_{crop} \tilde{r}_{mt} + \bar{\alpha}_{crop} + \xi_{crop,m,t}, \quad (12)$$

where \tilde{r}_{mt} is the only regressor measured in monetary units (in our case, Brazilian reais). We use its coefficient, α_{crop} , to give a monetary value to our counterfactuals.¹²

¹²An alternative observational equivalent presentation of our model would have $\alpha_{crop} = 1$, as the regressor is already measured in reais, but would allow for a dispersion parameter in the distribution of the logit shock

Pasture. A full structural model for pasture and livestock grazing is challenging given the essentially dynamic nature of cattle raising (see, e.g., Rosen et al., 1994). Here, instead, we propose a minimum structure for pasture flow profits that keeps some of the structure from the agriculture flow profit in equation (12):

$$r_j(w_{mt}; \alpha) = \alpha_{j,t}^1 y_{m,j} + \alpha_j^2 d_m y_{m,j} + \bar{\alpha}_j + \xi_{j,m,t} \text{ for } j = \text{pasture}, \quad (13)$$

where d_i is road distance to port and $y_{m,pasture}$ is a measure of pasture suitability. The returns of using the land for pasture depends on the interaction of suitability and prices, which are flexibly represented by a time-varying coefficient. Like agricultural products, livestock products must be transported to a destination market, so we use a structure reminiscent to the one for crops in which distance is interacted with suitability. Overall, we impose less structure to pasture flow profits, being considerably more flexible than for crops.

Forest. Finally, we model the return of leaving a field in location m unused to depend on the carbon stock of native vegetation h_m in that field. So, for $j = \text{forest}$, we have:

$$r_{\text{forest}}(w_{mt}; \alpha) = \alpha_{\text{forest}} h_m + \xi_{\text{forest},m,t}, \quad (14)$$

where h_m denotes the carbon stock in location m . The coefficient α_{forest} captures the combination of two elements. First, the effect of environmental protection policies targeted at forest preservation that are linked to forest density. It measures how much those policies help farmers internalize the value of the standing forest. Second, the private costs and benefits associated with forest density. On the cost side, higher levels of carbon stored indicate an area of dense forest that may be more susceptible to encroachment, since the delimitation of property may be blurred and more costly to enforce, resulting in potential loss of property rights or other damages (see, e.g., Hornbeck, 2010). On the benefit side, preserving an area with high carbon stock may be correlated with benefits such as protecting riparian forests and water springs. In our counterfactual carbon tax exercise, we will take into account these two possible interpretations: policies or private net benefits.

We have normalized the intercept $\bar{\alpha}_{\text{forest}}$ to zero. Therefore, other costs and benefits of keeping forests which are not related to forest density will be captured by the intercepts of pasture and crop returns and by the structural error $\xi_{\text{forest},m,t}$.

ε_{imjt} . When standardizing such model dividing all payoffs by the standard deviation of ε_{imjt} , the inverse of the standard deviation of ε_{imjt} would show up as a coefficient for \tilde{r}_{mt} . Thus, we can also interpret α_{crop} as the inverse of the standard deviation of the logit shock ε_{imjt} .

4 Data

4.1 Land use in the Brazilian Amazon

We obtain information on land use in the Amazon biome from MapBiomas.¹³ This data uses Landsat images to classify the use of each 30 meters resolution pixels in Brazil into several land use categories every year. We aggregate land use into four categories: crops, pasture, forest, and other (i.e., non-classified pixels, urban areas, and water). We exclude pixels in the other category and all protected areas from our sample.

The key element to build the dependent variable in our regression equation (9) is the conditional choice probability $p(j|k, w_{mt})$ – that is, the probability of transitioning from land use k to j conditional on location and time. We estimate this conditional probability non-parametrically. Even in a sample as big as ours, the curse of dimensionality in field characteristics implies that a full standard non-parametric attempt at estimating these conditional probabilities would be imprecise. We compute the conditional probability on the two geographical dimensions: latitude and longitude. This reduces the number of field characteristic dimensions being used. We believe this is a good compromise for land use applications because all field characteristic variables vary smoothly over space. For a given pair of years (e.g., 2008 and 2009) and a transition (e.g., crop to pasture), we build a matrix of zeros and ones, where one indicates that a 30-meter pixel made this transition between those years. This transition matrix has many zeros, as transition rates between some pairs of land uses are low.¹⁴ We then take the average of the nearby pixels reducing our dataset resolution from 30 meters to 1 kilometer.¹⁵ In addition, land-use decisions are highly correlated across space, so working with a coarser resolution attenuates efficiency issues arising from this spatial correlation.

We map this resolution coarsening directly into our model. The interpretation is that a 30-meters pixel represents a field – denoted by i in our model – and a 1-kilometer pixel represents a location – denoted by m – where our suitability measures ($y_{mc}, y_{m,pasture}$), transportation variables (z_{mc}, d_m), carbon stock (h_m) and most important the aggregate shocks ξ_{jmt} are homogeneous. This aggregation will be natural in our setting, given the resolution of the remaining variables explained in the next subsections.

Even at a 1-kilometer resolution, we still get many locations with close to zero transi-

¹³Project MapBiomas - Collection 4.0 of Brazilian Land Cover & Use Map Series, accessed on 20/01/2020 through the link: <http://mapbiomas.org>.

¹⁴This is partially depicted in Table 1, where we highlight the low transition rates between forest to crop. There will be less persistence over longer periods in transitions than a year to year, so we need to deal with transitions much lower than depicted in Table 1.

¹⁵We reduce the resolution of the data also for computational reasons.

tion rates. Those extreme conditional choice probabilities make it impossible to compute the Hotz-Miller inversion needed for model estimation. To deal with this, we smooth the probabilities of each location m by applying a Gaussian filter to the grid of locations.¹⁶ This is a technique commonly used for image processing to blur images and reduce noise. We provide additional details on the estimation of conditional choice probabilities in Appendix B.2. With the conditional choice probabilities in hand, we compute the dependent variable of (9), taken as given the discount rate ρ .

4.2 Field characteristics

We now detail the different land characteristics we use to model the flow profits under different uses in equations (12) to (14).

Carbon stock. We model the return of leaving the field i unused to depend on the carbon stock of native vegetation in 2000 (equation 14). Our carbon stock data comes from the Woodwell Climate Research Center, which provides values for 30 meters resolution of above-ground live woody biomass that we convert to the potential of CO_2 release (Zarin et al., 2016).¹⁷ For exposition purposes we will call this measure the carbon stock.¹⁸

The carbon stock data is key for our main counterfactual exercises as it gives us a measure of the location-specific social cost of deforestation – i.e., the carbon in that pixel released once deforested. Figure 2 shows the amount of carbon stock stored in the forest in 2000, the first year for which we have carbon stock data. One should expect that the carbon stored in areas that have been deforested to be smaller than the potential carbon that this same area could store once left idle for a long period. Therefore we restrict our sample to pixels outside protected areas that were not deforested before the year 2000, which amounts to 81% of the observations.

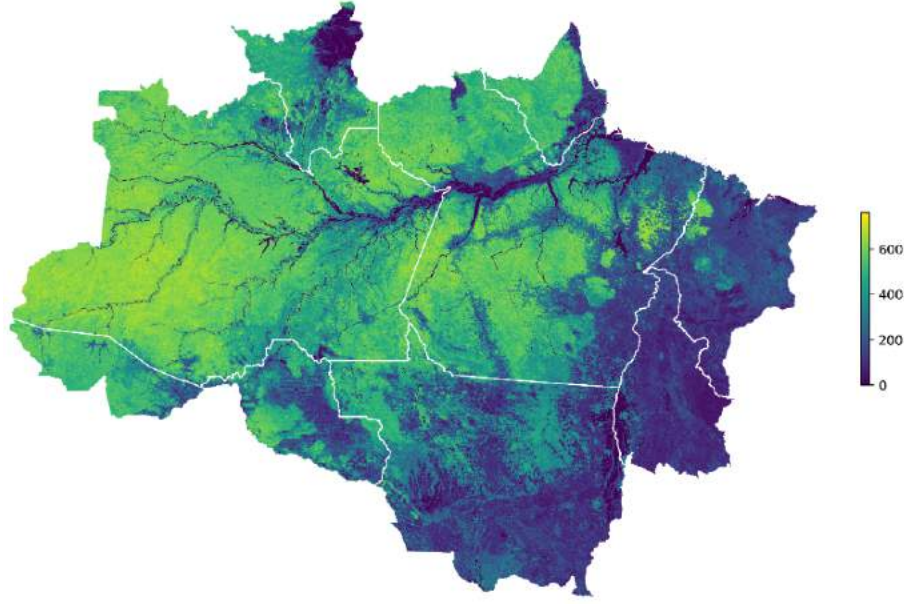
Potential crop returns. We model the return for crops specified in equation (12). That is, the return of crop in a field in location m in year t is the weighted average of the expected

¹⁶We set the standard error of the Gaussian distribution to 150 kilometers to eliminate most of zero transitions. When applying this filter, we ignore the transition coming from pixels inside protected areas.

¹⁷We only consider aboveground biomass because: (i) it comprises most of the biomass (about a fifth of the biomass of tropical forests are belowground, IPCC, 2019); (ii) we have no granular data for belowground biomass; and (iii) most types of forest clearing do not release the belowground biomass (Malhi et al., 2008).

¹⁸This dataset builds on the methodology of Baccini et al. (2012). The unit in the original data is megagram Biomass per hectare. To convert biomass to CO_2 per hectare, this value must be divided by 2 – giving a measure of carbon (C) – and then multiplied by 44/12 – giving a measure of carbon dioxide (CO_2). Accessed through Global Forest Watch Climate on 02/04/2020. <https://data.globalforestwatch.org/datasets/aboveground-live-woody-biomass-density>.

Figure 2: Carbon Stock in 2000



This map plots carbon stock density (tons of CO_2 per hectare) at 30 meter resolution. The values vary from blue (less carbon) to yellow (more carbon).

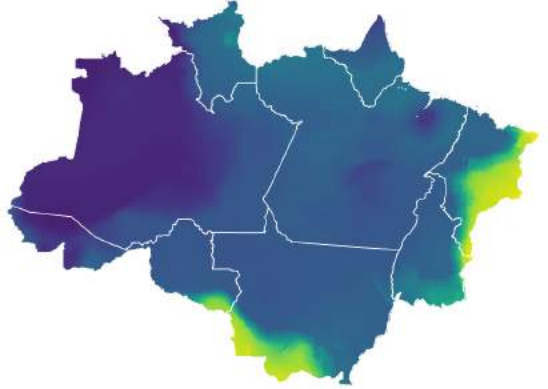
revenue from different crops in location m 's region, net of transportation costs to the nearest port. We consider soy and maize as possible crops, which constitute the bulk of cash crops produced in the Amazon. The weighting of these different crops is taken by the share of each crop in m 's mesoregion.¹⁹ The share of each crop comes from the 2006 Census of Agriculture sourced by the Brazilian Institute of Geography and Statistics (IBGE).

Potential yield for each crop is from the Food and Agriculture Organization's (FAO) project Global-Agroecological Zones, which provides crop-by-crop yields estimates at approximately 10 kilometers resolution. Those potential yields are given for a variety of scenarios, differing according to available inputs and water sources. We use the yields of high inputs, which FAO describes as the market-oriented agriculture production, and rainfed cultivation, the predominant form of production in the Brazilian Amazon. Figure 3a-b illustrate the potential yields for maize and soy. We see that there is substantial variation in soy suitability, although the East and Southwest regions are more suitable for maize. Last, to calculate the revenues of the potential yield, we use yearly maize and soy prices from the economic research center at the College of Agriculture Luiz de Queiroz (ESALQ).

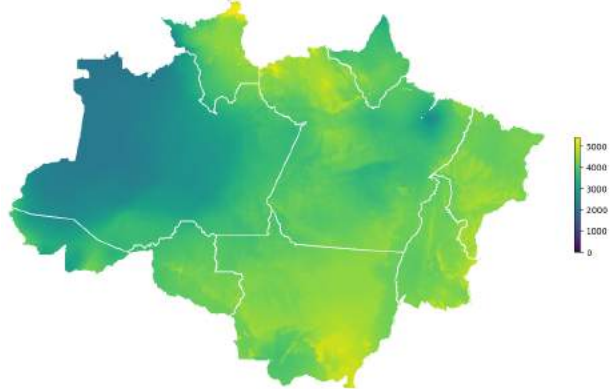
¹⁹A mesoregion is a classification from the Brazilian Institute of Geography and Statistics (IBGE) that groups contiguous municipalities with common geographic and socioeconomic characteristics.

Figure 3: Agricultural Potential Yield and Transportation Costs

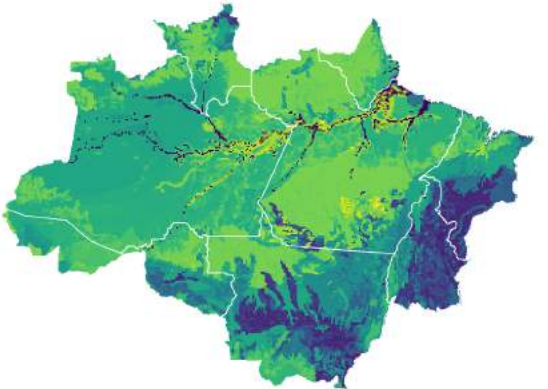
(a) Potential Yield Maize



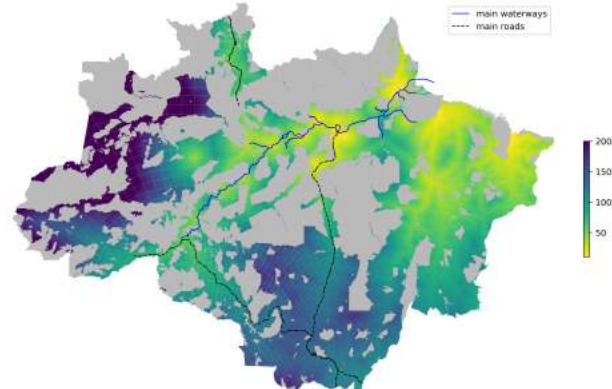
(b) Potential Yield Soy



(c) Pasture Suitability Index



(d) Transportation Costs for Soy



This figure plots the potential yield (kg per hectare) of maize (a) and soy (b), the index for pasture suitability (c) from FAO-GAEZ, and the minimum transportation costs of soybeans (d) from every pixel to the international market in reais (R\$) per ton – the values were capped at 200 for better visualization. Values vary from blue (lower) to yellow (higher).

Potential pasture returns. We model the location-specific return for pasture grazing by interacting potential pasture suitability with year dummies and the transportation costs to the nearest port (equation 13). We use the potential suitability index for livestock grazing from FAO illustrated in Figure 3c. Differently from our potential yield measures for soy and maize, the pasture suitability index is not a cardinal measure, i.e., it is not measured directly in units of output per hectare. Given the flexible pasture returns specification, we believe this non-cardinality is not a serious limitation.

Transportation costs. We estimate the cost of transporting agriculture products from each pixel to the nearest export port. While the literature calibrates these parameters, we

use a state-of-the-art data-driven approach. This requires several steps and data sources. We provide details on the technical procedures in Appendix B.1.

We first estimate the monetary cost of transporting agricultural goods on roads. To do that we combine georeferenced data on roads from the National Bureau of Infrastructure DNIT with internal freight costs of maize and soy collected by the Group of Research and Extension in Agroindustrial Logistics at ESALQ. For each pair of locations in the freight cost data, we compute road quality-adjusted distances for different relative transportation costs over pixels with roads (paved and unpaved) and without roads. We then regress freight costs on quality-adjusted distances by non-linear least squares as Donaldson (2018). This gives us the monetary cost of crossing land pixels featuring all types of transport infrastructure.

Second, we collect georeferenced data on all ports and waterways from the Ministry of Transportation to calculate the transportation cost by waterways, a commonly used transportation mode in the Amazon. We compute the minimum cost to ship products from every location to the nearest final port considering bi-modal transportation using Dijkstra’s shortest path algorithm. This produces a map with a monetary cost to transport each product from each location to an international port. Figure 3d plots the transportation cost of soy.

We compute the transportation cost for soybeans and maize – $z_{m,soybeans}$ and $z_{m,maize}$ in the model. For the pasture variables, we use the quality-adjusted distance – before the transformation to a monetary value via the freight cost regression – d_m in the model.

4.3 Summary statistics

We close this section by presenting summary statistics for the main cross-section variables used to estimate the model. Table 2 shows considerable cross-section variation in agricultural suitability and transportation costs. This variation is important because we are interested in counterfactuals with long-run shifts in agricultural returns. In our model, a permanent increase in prices, for instance, is equivalent to an increase in agricultural potential yields or a decrease in transportation costs. Thus, the cross-section variation on the net returns of crop and cattle grazing is key to calculating price elasticities based on the model.

5 Identification and Estimation

We estimate the structural equation (9) which relates the conditional choice probabilities and the potential returns of the different land uses in two steps. Because we want to allow for systematic differences across locations in the unobservables ξ_{jmt} , we first use standard panel

Table 2: Descriptive Statistics

Variable:	Potential yield			Transportation cost		Carbon Stock
	Maize	Soy	Pasture	Maize	Soybean	
Model analog:	$y_{m,maize}$	$y_{m,soy}$	$y_{m,pasture}$	$z_{m,maize}$	$z_{m,soy}$	h_m
Unit:	(ton/ha)	(ton/ha)	(index)	(R\$/ton)	(R\$/ton)	(ton/ha)
	(1)	(2)	(3)	(4)	(5)	(6)
mean	5.61	3.32	5115.26	103.53	102.42	310.20
std	1.43	0.59	2252.12	61.22	62.09	239.50
min	0.00	0.00	0.00	7.79	5.32	0.00
25th percentile	5.12	3.10	3923.00	57.20	55.43	34.83
50th percentile	5.33	3.52	5611.00	93.01	91.75	330.00
75th percentile	5.66	3.72	6672.00	137.72	137.10	537.16
max	10.63	4.54	10000.00	571.58	577.13	856.16

This table shows descriptive statistics for the field characteristics used in the model's estimation. Transportation costs are in reais ($R\$$) from 2008, the first year we have data on transportation cost.

techniques to estimate coefficients for time-varying regressors related to crop and pasture returns. We then estimate the remaining coefficients by OLS from the equation in levels.

5.1 First step: Within location estimation

We take differences over time in equation (9) to eliminate the fixed location specific component of ξ_{jmt} :

$$\Delta Y_{j,k,m,t} = \alpha_{crop} X_{j,k,m,t} + (\alpha_{pasture,t}^1 - \alpha_{pasture,t-1}^1) W_{j,k,m,t} + \Delta \zeta_{j,k,m,t}, \quad (15)$$

where the dependent variable $\Delta Y_{j,k,m,t}$ is a first difference of the dependent variable in equation (9):

$$\begin{aligned} \Delta Y_{j,k,m,t} &= \left[\log \left(\frac{p(j|k, w_{mt})}{p(k|k, w_{mt})} \right) - \rho \log \left(\frac{p(j|k, w_{m,t+1})}{p(j|j, w_{m,t+1})} \right) \right] \\ &\quad - \left[\log \left(\frac{p(j|k, w_{m,t-1})}{p(k|k, w_{m,t-1})} \right) - \rho \log \left(\frac{p(j|k, w_{mt})}{p(j|j, w_{mt})} \right) \right]. \end{aligned}$$

The regressors $X_{j,k,m,t}$ and $W_{j,k,m,t}$ are, respectively, the returns in difference for crop and pasture defined as:

$$X_{j,k,m,t} = \begin{cases} (\tilde{r}_{mt} - \tilde{r}_{m,t-1}) & , \text{ if } j = \text{crop and } k \neq \text{crop}, \\ -(\tilde{r}_{mt} - \tilde{r}_{m,t-1}) & , \text{ if } k = \text{crop and } j \neq \text{crop}, \\ 0 & , \text{ otherwise.} \end{cases}$$

$$W_{j,k,m,t} = \begin{cases} y_{m,pasture} & , \text{ if } j = \text{pasture and } k \neq \text{pasture}, \\ -y_{m,pasture} & , \text{ if } k = \text{pasture and } j \neq \text{pasture}, \\ 0 & , \text{ otherwise.} \end{cases}$$

Note that forest return is not in this equation because it does not vary across time. Finally, the error term is:

$$\Delta\zeta_{j,k,m,t} = [\eta_j^V(w_{mt}) - \eta_k^V(w_{mt})] - [\eta_j^V(w_{m,t-1}) - \eta_k^V(w_{m,t-1})] + [\xi_{j,m,t} - \xi_{k,m,t}] - [\xi_{j,m,t-1} - \xi_{k,m,t-1}].$$

This procedure, however, creates endogeneity in the regression (15) because the error term $\eta_j^V(w_{m,t-1})$ is a difference of expected and realized values, thus correlated with \tilde{r}_{mt} . To circumvent this identification issue, we follow Anderson and Hsiao (1981) and use lagged values of returns ($\tilde{r}_{m,t-2}$) as instrument for $X_{j,k,m,t}$.²⁰ This is a valid instrument since $\tilde{r}_{m,t-2}$ is information known at $t-1$, so uncorrelated with the expectational error $\eta_j^V(w_{m,t-1})$.

Prices are the only observed state variables that vary over time, therefore since we take differences in \tilde{r}_{mt} , variation in prices over time helps identifying this coefficient. However this is not the sole variation in \tilde{r}_{mt} that allows identification of the crop coefficient. In our formulation for the crop return, potential yields and crop shares magnifies the price effect, which generates substantial variation in the cross section of $X_{j,k,m,t}$ due to cross-sectional variation in potential yields and crop shares.²¹

Table 3 presents the results of estimating equation (15). The third column displays our baseline estimates. As expected, we estimate a positive α_{crop} coefficient, meaning that an increase in crop returns increases the likelihood of land being converted to crop. The results for the first stage, where we regress the returns variable in difference ($X_{j,k,m,t}$) on its lagged

²⁰We could, in principle, estimate the model using the Arellano and Bond (1991) estimator as Scott (2018). The difference of the two estimators is the asymptotic efficiency. Due to the size of our data set – we have 79,473,168 observations in our main specification –, efficiency is not a practical problem. Besides that, the size of our data set would make it difficult to implement Arellano and Bond (1991)'s estimator.

²¹From equation (11), $\tilde{r}_{mt} - \tilde{r}_{m,t-1} = \sum_{c \in C} s_{cm} y_{mc} (p_{ct} - p_{c,t-1})$, which will vary in the cross-section of locations m . Figure D.1 displays the cross sectional variation in crop return difference.

Table 3: Crop Flow Profit Coefficient

Regressor	Model Parameter	Estimate
(1)	(2)	(3)
$X_{j,k,m,t}$	α_{crop}	0.000386 (0.000014)
$W_{j,k,m,2011}$	$\Delta\alpha_{pasture,2011}^1$	0.000035 (0.000001)
$W_{j,k,m,2012}$	$\Delta\alpha_{pasture,2012}^1$	-0.000010 (0.000001)
$W_{j,k,m,2013}$	$\Delta\alpha_{pasture,2013}^1$	-0.000040 (0.000002)
$W_{j,k,m,2014}$	$\Delta\alpha_{pasture,2014}^1$	0.000031 (0.000002)
$W_{j,k,m,2015}$	$\Delta\alpha_{pasture,2015}^1$	-0.000056 (0.000001)
$W_{j,k,m,2016}$	$\Delta\alpha_{pasture,2016}^1$	0.000059 (0.000001)

This table shows the estimates of α_{crop} obtained in the second stage regression (equation 15) using Anderson and Hsiao (1981) estimator. Column 1 reports regressors, while Column 2 displays the corresponding model parameters from Section 3.2, equations (13) and (14). Standard errors in parenthesis were computed with block bootstrap with 1000 iterations in a grid of 25km by 25km. Number of observations: 79,473,168.

value in level ($\tilde{r}_{m,t-2}$) are presented in Table D.2.

5.2 Second step: Estimation in levels

We use the estimated $\hat{\alpha}_{crop}$ and $\Delta\hat{\alpha}_{pasture,t}^1$ to estimate the remaining parameters in equation (9) in levels by ordinary least squares. Table 4 shows the results. The variables composing the pasture return do not have a direct structural interpretation, since those variables are used to flexibly model the returns of livestock grazing.

Carbon stock coefficient. The coefficient attached to the field's carbon stock, instead, has an economic interpretation. The carbon stock variable has a positive coefficient, indicating that a higher stock of carbon in a plot of land decreases the likelihood of this plot being converted to other uses. By monetizing the carbon stock coefficient – *i.e.*, dividing it by $\hat{\alpha}_{crop}$ –, we estimate that farmers' perceived value of preserving carbon in the forest is equal to R\$ 1.50 per ton of CO_2 per year. Taking this benefit of preserving carbon stored at the present value using a 5% annual interest rate, we estimate a perceived value of carbon of

\$ 7.26 per ton of CO_2 .²² This perceived value reflects the effect of environmental regulation, making agents partly internalize the social value of the carbon stored in the forest, summed up with net preservation private benefits and costs. In any case, the perceived value of carbon is substantially smaller than most estimates of the social value of carbon, starting at US\$ 18.50/ton (Nordhaus, 2014) and centered around US\$ 50/ton (EPA, 2016, value in 2030). That is, our estimates suggest that farmers when choosing to deforest do not take into consideration the full social costs of their action.

Table 4: Forest and Pasture Flow Profits Coefficients

Regressor	Model Parameter	Estimate	$/\alpha_{crop}$
(1)	(2)	(3)	(4)
h_m	α_{forest}	0.000580 (0.000027)	1.50 (0.12)
$W_{j,k,m}$	$\alpha_{pasture,2011}^1$	0.000064 (0.000001)	-
$W_{j,k,m}d_m$	$\alpha_{pasture}^2$	-0.000001 (0.0000001)	-
Intercepts			
	$\Phi(pasture, forest)$	-0.622 (0.001)	-1614.54 (62.18)
	$\Phi(crop, forest)$	-0.968 (0.004)	-2511.25 (94.54)
	$\Phi(crop, pasture)$	-0.596 (0.004)	-1547.21 (57.53)
	$\Phi(pasture, crop)$	-0.200 (0.002)	-519.02 (21.71)
	$\bar{\alpha}_{pasture}$	0.178 (0.003)	464.23 (21.25)
	$\bar{\alpha}_{crop}$	-0.587 (0.036)	-1523.52 (39.52)

This table presents the OLS estimates of equation (9), using $\hat{\alpha}_{crop}$ and $\Delta\alpha_{pasture,t}^1$ estimated in equation (15) using Anderson and Hsiao (1981). Column 1 reports regressors, while Column 2 displays the corresponding model parameters from Section 3.2, equations (13) and (14). Standard errors in parenthesis were computed with block bootstrap with 1000 iterations in a grid of 25km by 25km. Number of observations: 79,473,168.

²²We use the exchange rate of R\$ 4.14 per USD \$ from December 2019.

Transition costs. Finally, we also recover the conversion costs, $\Phi(j, k)$, and choice specific constants, $\bar{\alpha}_j$, from the transition specific intercepts of the regression (7) in levels.²³ Table 4 shows the recovered parameters. The conversion costs are all internally consistent. We estimate that the transition costs of clearing forest to grow crops is larger than clearing the forest to grow pasture. This is also intuitive as preparing the land for agriculture after clearing the forest requires more investments in the land (such as removing stumps, and leveling the terrain) than when preparing a pasture. Furthermore, the transition costs of clearing forest land to grow crops is close to the sum of the transition costs from forest to pasture and the transition from pasture to crop²⁴.

6 Counterfactuals

In this section, we use our estimated model to assess the carbon-efficient forestation and to discuss alternative policies to mitigate inefficient emissions. The value function for each alternative scenario is the key ingredient that needs to be computed to obtain the counterfactual conditional choice probabilities (CCP) using equation (5).²⁵ This computation of the value function needs to be performed numerically and is slowed down by the size of the state space. We make an important simplification: we remove all uncertainty about location specific state variables (w_{mt}) in the model – i.e., we set $w_m = \frac{1}{T} \sum_t w_{mt}$. The logit errors assumption implies that the integrated Bellman equation has a convenient expression:

$$\bar{V}(k, w_m) = \log \left(\sum_{j \in J} \exp (\Phi(j, k) + r_j(w_m; \alpha) + \rho \bar{V}(j, w_m)) \right) + \gamma, \quad (16)$$

where γ is the Euler constant.

²³We have six transition specific coefficients $\tau_{j,k}$ for $j \neq k$, which are related to model parameters through the system of equations:

$$\tau_{j,k} = (1 - \rho)\Phi(j, k) + \bar{\alpha}_j - \bar{\alpha}_k, \text{ for } j \neq k.$$

We have normalized $\bar{\alpha}_{forest} = 0$, so we have only two free $\bar{\alpha}_j$. Moreover, Assumption 4 implies we have only four free $\Phi(j, k)$. Therefore the system above just identifies conversion costs, $\Phi(j, k)$, and choice specific constants, $\bar{\alpha}_j$, given knowledge of ρ .

²⁴The estimates of land use conversion are in line with values found in case studies and specialized news: (i) computes a conversion cost of forest to pasture of R\$1,500/ha; (ii) and (iii) report a conversion cost of pastureland to cropland of R\$2,000/ha and R\$2,500/ha, respectively; and (iii) estimates a cost to deforest and convert land to soybeans production of R\$3,100 in (3).

(i) amazonia2030.org.br/wp-content/uploads/2021/09/pecuaria-extrativa_final_Paulo-Barreto-1.pdf

(ii) canalrural.com.br/projeto-soja-brasil/conversao-de-pasto-em-lavoura-de-soja-pode-triplicar-o-valor-da-terra

(iii) https://www.agroicone.com.br/wp-content/uploads/2020/01/TNC_IncentivesforSustainableSoyinCerrado_Nov2019.pdf

²⁵Note that estimation is performed without the need to solve for the value function. This is a convenient feature of Scott (2018)'s approach, which is shared by many other commonly used dynamic discrete choice estimators (e.g., Hotz and Miller, 1993; Aguirregabiria and Mira, 2007; Kalouptsidi et al., 2021).

After computing $\bar{V}(j, w_m)$ by iteration, we use expressions (3) and (5) to compute the CCPs. We then compute the invariant distribution for each location m , which gives a steady-state probability of one pixel in m being in a specific state: $A_m(j, w_m)$. Aggregating for all locations, we obtain the total steady-state land use, which we call $A(j, w)$, where $w = \{w_m\}_m$. This object is the basis for our counterfactual exercises.

6.1 Long-run effects of higher agricultural prices

In our first counterfactual exercise, we assess how a variation in agricultural prices affects land use and carbon release. Although this counterfactual is only indirectly linked to our main research questions, it is of interest on its own and helps situate our results in the wider literature. Here, we compare the steady state land use with (\tilde{w}) and without (w) a $100 \cdot \Delta\%$ price change and compute a long-run elasticity of land use with respect to agricultural prices:

$$\partial_{j,\Delta} = \frac{A(j, \tilde{w}) - A(j, w)}{A(j, w)} \frac{1}{\Delta}. \quad (17)$$

Table 5: Long-run Land Use Elasticities with Respect to Crop and Cattle Prices

	Forest Cover (1)	Crop Are (2)	Pasture Area (3)	Carbon Released (4)
Panel A. Crop price elasticities				
-0.45 (0.02)	6.3 (0.05)	-0.23 (0.01)	0.11 (0.01)	
Panel B. Cattle price elasticities				
-1.64 (0.04)	-0.45 (0.02)	1.34 (0.04)	1.66 (0.07)	

This table presents long-run elasticity of forest cover, crop area, pasture area and carbon released with respect to an crop price (*Panel A*) and with respect to cattle price (*Panel B*). Elasticities calculated with $\Delta = 10\%$ (eq. 17) price increase. Standard errors in parenthesis were computed with block bootstrap with 1000 iterations in a grid of 25km by 25km.

Table 5 Panel A reports land use elasticities with respect to crop prices. We estimate an own land-use price elasticity of 6.3 for cropland (column 2). Although this is high compared with evidence for the US reported in Scott (2018), it is in the ballpark of similar measures in the context of Brazilian agriculture, e.g., Sant'Anna (2021). We can also see that, although the cross elasticity of pasture with respect to crop price is relatively high (-0.23), most of the cropland increase is over the forest. Our model estimates an elasticity of forest cover with respect to agricultural prices of -0.45. These results are consistent with the literature arguing

that market conditions increase the pressure from agriculture over forest land in areas where the agriculture frontier is non-consolidated,²⁶ as common in countries with tropical forests.

In the fourth column of Table 5, we compute the effects of the price increase in the amount of carbon released under the assumption that all carbon stock in aboveground biomass is released by deforestation. That is, we sum the carbon stock of all plots weighted by the probability that each plot will be converted from forest to other uses in the counterfactual exercise. We estimate that the elasticity of carbon released with respect to crop prices is 0.11. This means that an increase of 10% in crop prices results in an additional 0.5 gigaton of CO_2 released in the steady state, amounting to \$25 billion of costs if we consider a social cost of carbon of \$50 per ton of CO_2 (EPA, 2016).

Table 5 Panel B reports land use elasticities with respect to cattle prices. We estimate a positive own land-use price elasticity (column 3), but smaller than the cropland own price elasticity. Although we observe the conversion of cropland to pastureland (the cross elasticity of cropland with respect to cattle prices is -0.45), the main change in land use is the conversion of forest to pasture. We estimate a cross elasticity of forest cover with respect to cropland of -1.64, and a cross elasticity of carbon released of 1.66. These elasticities are substantially larger than the cross elasticities with respect to crop prices. This suggests that changes in the market conditions of cattle have a greater impact on the forest than similar changes in crop markets. We return to this point when we discuss a tax on cattle production.

6.2 Efficient forestation

The socially optimal forest cover is the one in which agents fully internalize the externalities associated with deforestation when making land-use choices. In our main counterfactual exercise, we quantify the Amazon's efficient forestation in the steady state when agents internalize the social cost of carbon stored in each plot of forest. We do so by equating agents' private perceived value of the carbon stored in the forest to the social cost of carbon of \$50.00 per ton of CO_2 for the year 2030 (EPA, 2016).²⁷

We calculate that the steady-state efficient forestation under a social cost of carbon of \$50/ton would imply 44 gigatons less of CO_2 released into the atmosphere (95% confidence interval: 42.2 to 47.4) relative to the business-as-usual (BAU) steady state.²⁸ This corresponds to additional 1,075,059 km^2 in forest cover (95% confidence interval: 1,027,059 to 1,123,703) relative the BAU. Remember that our sample includes pixels outside protected

²⁶E.g., Assunção et al. (2015); Souza-Rodrigues (2019); Harding et al. (2021).

²⁷We consider 2030 because our counterfactual computes the steady-state land use, rather than the current short-run land use.

²⁸For each location m , we compute the steady-state 'forest' land use probabilities in both BAU and efficient

areas that were not deforested prior to 2000. In the BAU steady state, we estimate that only 47% of the stock of carbon in our sample is preserved. We find that the efficient forestation preserves about 99.5% of the carbon stock and 90.3% of the forest cover in our sample.

When we equate agents' perceived carbon value to \$50, we implicitly assume that our perceived value estimate reflects only the effect of policies and not private benefits and costs. In the other extreme case, in which the perceived value reflects only private factors and policy plays no role, we should bring agents' perceived value to $\$50 + \$7.26 = \$57.26$. However, as 99.5% of the carbon stock is already preserved when the perceived value is \$ 50, any higher value would imply no significant gains on preserving carbon. Similarly, potentially higher values for the social cost of carbon would also not bring substantial additional savings.

We can benchmark the magnitudes of our estimates relative to the deforestation process over the last twenty years. Hansen et al. (2013) forest loss data shows that around 565,343 km^2 was deforested in the Brazilian Amazon between 2001 and 2019. De Azevedo et al. (2018) calculates that land-use change in Brazilian Amazon in this period released 20 gigatons of CO_2 . Thus, achieving the additional 1 million km^2 of forest cover and preserving 44 gigatons of CO_2 in the efficient steady state means ceasing the current deforestation pattern for the next four decades. Alternatively, it means regenerating most of the deforestation that took place over the last twenty years and stopping deforestation for the next twenty years. In sum, implementing the first-best forestation is a Herculean task. In the rest of this section, we show how policies can help us to get closer to this efficient forestation.

6.3 Preserving the forest through carbon tax

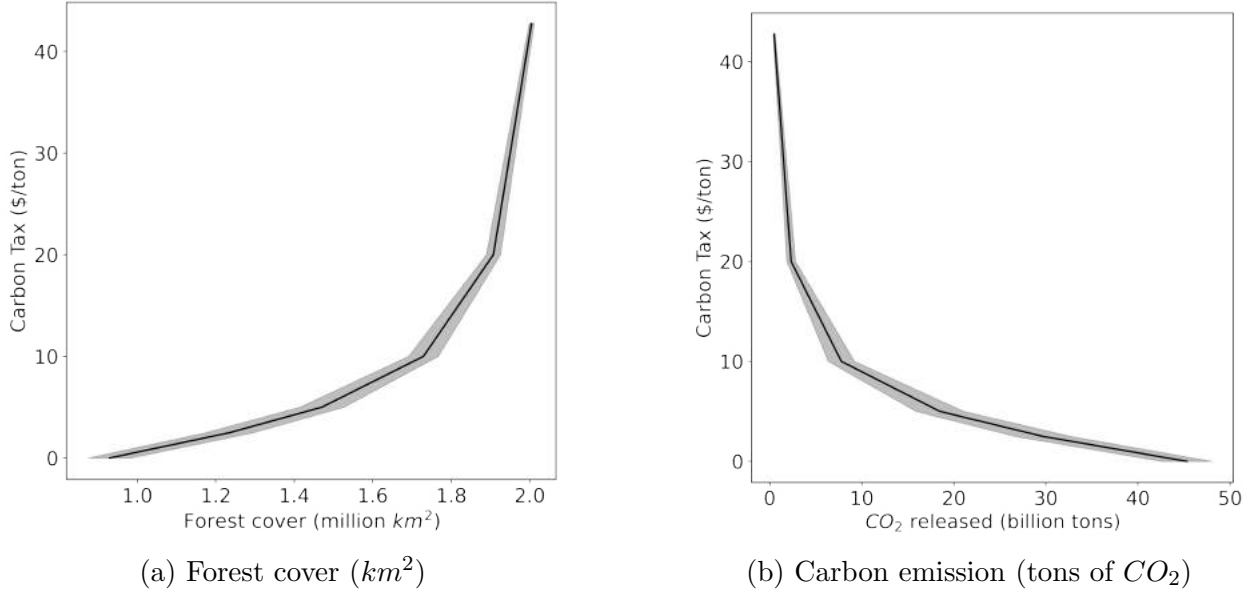
We now consider how a carbon tax based on the carbon content of the land could shape farmers' incentives and promote forest conservation. In this set of counterfactuals, we strengthen conservation policies by adding a carbon tax to be paid if the agent chooses to convert the forest to other use. Precisely, we increase the perceived return of preserving carbon in the forest α_{forest} , which is equivalent to providing a flow of payments for ecosystem services for preserving the forest (e.g., Alix-Garcia et al., 2015; Jayachandran et al., 2017; Wong et al., 2019). We interpret the present value of this flow as a carbon tax that can be compared to current measures of the social cost of carbon. We can also interpret the increase in the perceived value of carbon driven by stronger enforcement of environmental policies – such as

scenarios and assess excess emissions:

$$\Delta CO2_m = (A_m(forest, w_m^*) - A_m(forest, w_m)) h_m,$$

where $A_m(forest, w_m^*)$ and $A_m(forest, w_m)$ denote the steady-state probability of forest, respectively, in the efficient and in the BAU scenarios. Total emissions are just the sum of $\Delta CO2_m$ across all locations.

Figure 4: Forest Cover and Carbon Emissions by Carbon Taxes



This figure shows the steady state forest cover (a) and carbon emissions (b) for different values of carbon tax. Our baseline perceived carbon value implied by the model estimates is \$7.26 per ton of CO_2 . Here, we consider carbon taxes added to the baseline perceived value of carbon. The gray shaded area shows the 95% confidence interval computed using block bootstrap with 1000 iterations for a grid of 25km by 25km.

using remote sensing data to detect deforestation (Assunção et al., 2017) and rural registries to increase compliance (Alix-Garcia et al., 2018) – as a carbon tax in our model.

We calculate steady-state land use in different scenarios considering the inclusion of carbon taxes ranging from \$0/ton to \$42.74/ton, the tax that implements the efficient forestation level.²⁹ Figure 4 (and Table D.3) reports the results. The figure on the left shows the amount of forest cover (on the horizontal axis) under different carbon taxes (on the vertical axis), and the figure on the right shows the amount of carbon released for different values of a carbon tax. The main lesson from this figure is that there is a strong non-linearity in the amount of carbon release implied by carbon taxes, with relatively small carbon taxes closing a substantial share of the gap between the BAU and the efficient forestation. For example, a carbon tax of \$2.5/ton would preserve 15 gigatons of CO_2 (and 306 thousand km^2), leading the forest 34% [=15/44] closer to its efficient forestation. In the steady state, a carbon tax of \$10/ton would preserve 84% [=37/44] of the efficient carbon stock. This convexity is intuitive: it is relatively cheaper to preserve carbon deeper in the forest, as both carbon stock and transportation costs are higher. As the marginal land being preserved comes closer to the agricultural frontier (lower transportation costs), it becomes increasingly

²⁹42.74 (tax) + 7.26 (estimated perceived private value) = 50 (social cost of carbon).

costly to preserve carbon. A second intuition for this convexity is that land is the main input for the expansion of cattle ranching, so relatively small increases in the perceived cost of deforestation represent a substantial increase in the cost structure of expanding pastureland.

Figure 4b also shows that most of the conservation gains are achieved with carbon taxes under \$20/ton. Above this point, additional reductions in carbon emissions become increasingly costly. This is in line with the estimates of Souza-Rodrigues (2019) that find that a carbon tax of \$18.50/ton would make farmers in the Amazon indifferent between producing or preserving the forest. Note, however, that even in the efficient steady state we observe about 9% of our sample being used as pastureland or cropland.

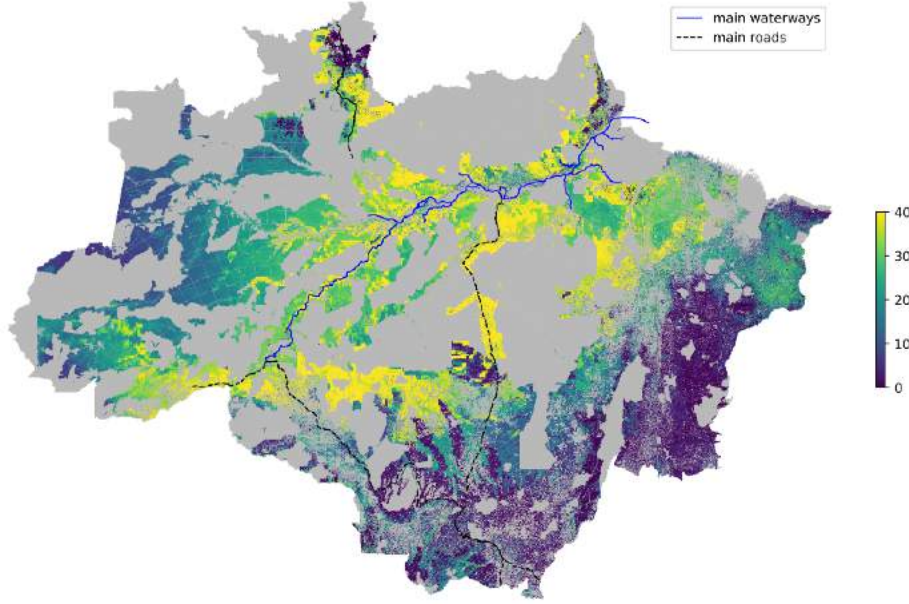
6.4 Spatial targeting of carbon tax

Many policies aimed at reducing deforestation are based on some sort of spatial targeting. The spatial dimension was a key element in the main policies implemented in the Brazilian Amazon in the 2000s. For example, the creation of new protected areas (Soares-Filho et al., 2010; Nolte et al., 2013), the implementation of the DETER system that uses satellite images to identify deforestation hot spots and guide command-and-control missions (Assunção et al., 2017; Ferreira, 2021), and the creation of a list of priority municipalities that would be under stronger scrutiny (Assunção and Rocha, 2019). We exploit the spatial heterogeneity in the private returns and the social cost of deforestation to investigate the potential of policies based on geographical targeting.

First, we use the spatial granularity of the data to map the pixels in which the inefficient loss of carbon would be more severe. Figure 5 displays the excess of emissions in the BAU relative to efficiency in each location. The difference between efficient and BAU carbon holdings reach up to 40,000 tons of CO_2 per km^2 in some locations, a social loss of \$2 million per km^2 . Those areas are especially around main waterways and roads in the state of Pará. This large gap is due to a combination of high carbon density (which drives up efficient forestation) and low transportation costs (which drives down forestation in BAU). Meanwhile, darker regions represent places in which the BAU is closer to efficiency. Those are areas with small carbon stock (on the Amazonian fringe) in the states of Mato Grosso and Tocantins, and areas in the far west in which even though carbon stock is high, transportation costs are prohibitive. This heat map can be a useful tool for the design of cost-effective targeted conservation policies.

We use our model to quantify the effectiveness of strengthening regulation and enforcement only in areas with the greatest potential for emission reductions. We consider scenarios where we implement different values of carbon taxes only on pixels with the largest potential

Figure 5: Geographical Distribution of Inefficient Emissions in Steady State



This map displays emissions in the BAU scenario (perceived carbon value of \$7.26) in excess of emissions in the efficient scenario (perceived carbon value of \$50) for each pixel.

for reductions in carbon emissions. Specifically, for each value of carbon tax, we rank pixels according to their reduction in steady state emissions. We then compute scenarios where we impose the carbon tax only on those pixels with greater potential for reduction.³⁰

Table 6 shows the results of this exercise. We find that targeting the carbon tax on the 25% of pixels that generate the largest emission reduction would preserve more than half of the emissions as compared to the same tax implemented in the whole region. For example, a \$2.5/ton and \$10/ton carbon tax targeted at the top quartile would mitigate the emissions of 8.9 gigatons and 19.7 gigatons of CO_2 in the steady state, respectively. Our results also indicate that targeting at the very top is also effective. For example, targeting at the top 1 and 2 percentiles of pixels with greater potential reductions would preserve 3% and 6% of the carbon preserved by the tax implemented in the whole region, respectively.

While some policies can be targeted at the pixel level (e.g., zoning and monitoring with remote images), others may be expensive to implement at such a granular level. Nonetheless, our model can inform the spatial placement of policies at a more aggregate level. For example, policies at the municipality level were implemented in 2008 when the Brazilian government

³⁰Notice that there is no spatial leakage in this exercise because taxing pixel i does not change the returns of pixel j . In other words, pixels not deforested are those in which crops or cattle are not profitable, and this is not affected by policy elsewhere. The only potential leakage would be through general equilibrium price changes. In Section 7.2, we show that general equilibrium effects are likely to be small in our setting.

Table 6: Targeted Carbon Tax on Released Gigatons of CO_2

Carbon tax (\$/ton)	Percentile (%)					
	1	2	5	10	25	100
	(1)	(2)	(3)	(4)	(5)	(6)
2.5	-0.5	-1.0	-2.2	-4.2	-8.9	-15
5.0	-0.8	-1.6	-3.7	-7.0	-14.8	-26
10.0	-1.1	-2.1	-4.8	-9.1	-19.7	-37
20.0	-1.1	-2.2	-5.1	-9.7	-21.4	-42

This table shows the difference of CO_2 emissions in comparison with the business-as-usual steady state. For each different carbon tax (rows) we identify the pixels that would save more emissions according to different percentiles (columns). We then consider the result of imposing the carbon tax only on those pixels. Column (6) presents the baseline case of a carbon tax implemented in the whole area as in Table D.3.

created a Priority List of municipalities with greater past and current deforestation activity (Assunção et al., 2019b). We identify in our model the municipalities likely to produce more inefficient emissions by ranking them according to their average excess of emissions in the BAU relative to the efficient level. If we apply the efficient carbon tax only to 52 highest ranked municipalities – to keep the same number of municipalities as in the actual Priority List –, 11% of the pixels in our sample would be targeted and the release of 9 gigatons of CO_2 would be avoided. Table D.8 lists these 52 municipalities with their respective average emissions, and Figure D.2 maps them.

6.5 Preserving the forest through taxes on cattle ranching

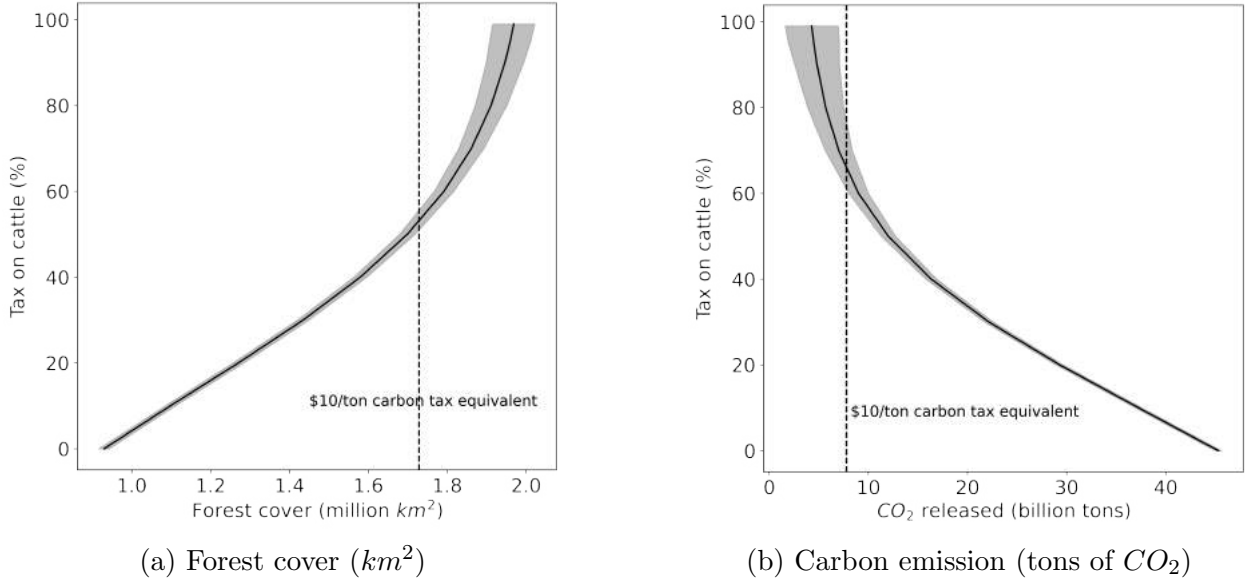
We now assess the potential effects of excise taxes on cattle ranching and crops to promote forest conservation. There are increasing discussions on how market interventions, such as international tariffs (Abman and Lundberg, 2020; Hsiao, 2021) or bans on goods produced in areas under deforestation pressure (e.g., Nepstad et al., 2014; Harding et al., 2021). We, therefore, compute the steady-state land use under scenarios where agents are subject to taxes on cattle or crop goods – i.e. an *ad valorem* tax on the return of cattle ranching or crops.

Figure 6 displays the results of different tax levels on the return of cattle ranching (vertical axis) on forest cover (a) and carbon emissions (b). We find that the relationship between cattle taxes and carbon emissions is also convex, however not as much as carbon taxes. Figure 6b shows that relatively smaller taxes, such as a 20% rate, can save about 16 gigatons of CO_2 .³¹ A 65% tax on cattle is necessary to save the same amount of carbon as a \$10/ton

³¹Note that we only consider emissions from the carbon released by deforestation, not the methane pro-

carbon tax – marked with a vertical dashed line in the figure. We see a similar pattern in Figure 6a that displays the amount of forest cover for each level of a cattle tax. It shows that a 53% tax on cattle induces the same extent of forest cover in the steady state as the one implied by the \$10/ton carbon tax. We also experimented with a tax on crops, but we find that the tax on crops produced only marginal changes in carbon emissions.

Figure 6: Effects of a Cattle Tax on Forest Cover and Carbon Released



This figure shows forest cover (a) and carbon emissions from deforestation (b) for different levels of excise taxes on cattle ranching. Dashed lines highlight forest cover (a) and carbon emissions (b) that would follow from a \$10/ton carbon tax for comparison across policy exercises. The gray shaded area shows the 95% confidence interval computed by using block bootstrap with 1000 iterations for a grid of 25km by 25km.

In sum, the low productivity economic activities currently in place in the region and the large amounts of carbon stored in the forest make a relatively small strengthening of environmental policies (i.e. small carbon taxes) go a long way in bringing the Amazon closer to the efficient forestation. On the other hand, current small opportunity costs of preserving the forest make small returns from deforestation, such as converting to extensive cattle ranching, privately economically attractive. Thus, only large excise taxes can disincentivize forest conversion to the extent needed to mitigate inefficient carbon emissions from deforestation.

duced by the cattle.

7 Caveats and extensions

Our analysis relied on assumptions and simplifications that may impact our conclusions. In this section, we discuss the main caveats when interpreting our results and present extensions.

7.1 Forest regeneration

Our baseline model features a direct transition between crop and pasture to the forest state. When assessing carbon emissions, we assumed the aggregate steady state forest cover holds its full carbon stock potential. Nonetheless, fields may be constantly changing their land use and fields that return to the forest state may take decades to recoup their carbon potential by natural regeneration.³² This will not matter for the carbon tax counterfactual, since we assume the tax is implemented over the potential carbon stock, but it may be important for long-run emissions.

To assess how sensitive our results are to this simplification, we consider an extreme opposite scenario for carbon accounting as robustness. We assume that a field converted to ‘forest’ holds zero carbon in the first 30 years. After 30 years, the full stock is recovered.³³ Table D.7 displays the results for released carbon and avoided emissions from the carbon tax and compares them to our baseline specification. In this extreme scenario, there are naturally more carbon emissions in the long run since a higher share of forest under regeneration is not holding any carbon. However, the amount of avoided emissions from modest carbon tax policies are similar to our baseline. For instance, a \$10/ton carbon tax saves 37.5 gigatons relative to BAU in our baseline (Table D.3) and 42.4 gigatons in this extreme exercise. For stronger policies, the difference between the exercises increase and the efficient carbon pricing would imply 62 Gt CO_2 fewer emissions, compared to 44 Gt CO_2 in our baseline. These results suggest that a more complete forestry modeling should not be a game-changer to evaluate modest policy changes, but they also suggest our baseline specification may underestimate the efficient carbon gap.

7.2 Equilibrium effects

In our analysis, we ignore possible equilibrium effects from the policies considered. This is valid if agricultural commodities here are internationally traded and this region represents a

³²Forest biomass regeneration is faster at the beginning of the regeneration process and slows down over time. After 25 years, it recoups 70% of its original biomass (Houghton et al., 2000).

³³We provide details for this exercise in Appendix B.3.

small share of the supply,³⁴ being insufficient to affect world prices. However, if this condition is not valid, an efficient carbon tax on deforestation or a tax on beef would decrease the supply of these commodities and push world prices up.

A simple back-of-the-envelope calculation suggests a small 1.9% world beef price increase from implementing our efficient land use in the Amazon.³⁵ This price increase could partially offset the decrease in deforestation by increasing acreage as we move to a new market equilibrium, as well as harming consumers worldwide. Given our estimated cattle supply elasticity of 1.34, this acreage offset would be limited to 2.6% of the cattle grazing area. Because only 2% of the region is cropland and a small share of Brazilian soybeans are harvested in the Amazon, the general equilibrium effects of crops would be even smaller.

7.3 Externalities beyond carbon

We only look at carbon emissions when computing the social cost of deforestation. This ignores the potentially big externalities involved in the loss of biodiversity that follows deforestation. Moreover, there has been a recent discussion on how the loss of green cover may change rain patterns, leading to disruptions in agriculture and even to a complete transformation of the vegetation landscape.

Extracted water from tree roots returns to the atmosphere by transpiration, being responsible for 25 to 50% of the rainfall in the Amazon (Malhi et al., 2008). This recycled water is critical for the forest's existence, as another drier savanna equilibrium is possible in this region (e.g. Staver et al., 2011). In fact, recent research suggests that large-scale deforestation beyond a tipping point – about 40% of the original forest – may trigger a self-propagating transition to savanna (Franklin Jr and Pindyck, 2018).

In our long-run BAU steady state, we have deforestation of 58% of our sample, which does not include protected areas. Assuming, that in the long run all existing protected areas remain intact and there is no regeneration of fields deforested before 2000, total deforestation of the Amazon in the BAU steady state would be 31%, still short of the 40% tipping point. However, this result is highly dependent on the preservation of protected areas, which is crucial to avoid long-term permanent changes to the biome (Soares-Filho et al., 2006, 2010).³⁶

³⁴In 2018, Brazil accounted for 10% of global cattle production, 7% of global maize, and 34% of global soybeans (FAOSTAT).

³⁵The Brazilian Amazon accounts for 4.1% of the beef world supply (FAO and IBGE) and our efficient land use implies a reduction of 84.8% in the area devoted to cattle grazing, implying a 3.48% reduction in world supply. Assuming the supply elasticity across the globe is the same as the one we compute for the Brazilian Amazon (1.34) and demand elasticity of -0.45 (Brester and Wohlgemant, 1993), we find a small world price equilibrium effect of $1.9\% = 3.48\% / (0.45 + 1.34)$.

³⁶Our model is not designed to project land use in these areas. While we acknowledge that the assumption

All these unmodelled effects are potentially big, but we know of no study explicitly computing social costs arising from these effects that we could directly apply to our setting. Therefore, we decided on the conservative approach of only factoring in social costs related to the release of carbon stored in the forest. However, we conjecture that these other externalities we cannot account for are all negative, making the optimal forest gap even larger once those are explicitly factored in.

7.4 Technology

We study the steady-state equilibrium choices under the current technologies used in agriculture and cattle ranching in the Amazon. If farmers in the region slowly adopt more productive technologies over time, in the long run, the returns of agriculture will be higher. As robustness, we estimate an extension of the model where we model the return of agriculture using the most productive technology available in nearby regions in Brazil. Specifically, we consider that every pixel produces crop with a double-crop system, producing soybeans in the main season and maize for the second season in the same agricultural year, and consider the high inputs scenario for soil suitability (e.g., Bustos et al., 2016).

Column 1 in Tables D.4 and D.5 show the estimates with double cropping. In this setting, we estimate a perceived value of carbon of \$ 16.29/ton of CO_2 . This is larger than our baseline estimates because rationalizing the amount of forest seen in the data with a higher crop return requires a higher forest return. Nonetheless, this perceived value of carbon is still substantially smaller than the social cost of carbon.

We estimate that the efficient steady state would prevent 37 gigatons of CO_2 from being released to the atmosphere relative to the BAU steady state. Table D.6 Panel A shows the counterfactual forest cover and CO_2 released under the different carbon taxes. We still see a convex relationship between the carbon price and emissions, but slightly less than in our main estimates in Table D.3. For example, a \$10/ton carbon tax saves 67.6% of the efficient carbon emissions in the steady state with a double crop.

7.5 Technical assumptions

Discount rate. As in most applications, we do not estimate the discount factor as it is poorly identified (Rust, 1994). We re-estimated the model and counterfactuals with a discount factor of 0.95 (our baseline uses 0.90). Results for main counterfactuals of interest are

that protected areas will be preserved is quite strong, any other assumption on the long-run trends of land use in these areas would be outside the model and, therefore, similarly strong.

reported in Table D.6 Panel B. The more patient discounting implies that a lower perceived carbon value of \$5.72 per ton of CO_2 is sufficient to rationalize the observed land use. This implies a bigger gap in the social value of carbon, resulting in a bigger carbon gap between efficient and BAU scenarios. A \$10/ton carbon tax, for instance, would imply 24% more carbon saved under this more patient model than in the baseline.

Counterfactual simulations. There are a few caveats in our counterfactual simulations that merit discussion. First, when we compute the long-run steady state we abstract from uncertainty in commodity prices and other market variables (Cai and Lontzek, 2019). The estimation method we employ allows us to be agnostic about how farmers perceived transitions for those state variables. Therefore, incorporating uncertainty in counterfactual simulations would require us to make additional assumptions and empirical work. This simplification also challenges the interpretation we could derive from transitions to the long run. For this reason, we also limited ourselves to comparing steady-states. Nonetheless, we believe that our exercise captures the main trade-offs between production and preservation in the long run.

8 Conclusion

In this paper, we estimated the efficient level of carbon storage in the Brazilian Amazon forest using an original dynamic discrete choice model where farmers make decisions on land use. We used the estimated model to compute the long-run gap between the optimal forest and the one we will have under status quo practices and policies. We find that such a gap is large as farmers currently value the carbon stored in the forest at \$7.26 per ton of CO_2 , which is substantially smaller than current estimates of the social cost of carbon released to the atmosphere (EPA, 2016, e.g., estimates a social cost of carbon in 2030 of \$50.00/ton).

We also used the model to quantify how the introduction of a carbon tax to land use or excise taxes on cattle ranching and crops can help to close, at least partially, such a gap. We find a very convex response of carbon emission from deforestation to carbon taxes, such that relatively small carbon taxes can mitigate a substantial part of inefficient emissions. We show that our granular estimates can be used to think about targeted policies. Targeting policies on areas with greater potential for emission reductions can be very effective. Our counterfactuals also show that while crop taxes have virtually no effect on forestation, taxes on cattle raised in the Amazon can be effective in partially closing the efficiency gap.

Our results highlight the stark change in economic incentives needed to mitigate inefficient

emissions from land use in the Amazon. While the logistics of implementing such policies are not simple, we understand that Brazil has demonstrated that it can use technology to enforce environmental compliance and that there is a will from the international community to help fund it. On market side policies, we find that disincentivizing the main driver of deforestation in the region – cattle grazing – can also be effectively used to reduce inefficient deforestation in the long run. Technologies such as cattle tracing and a moratorium on Amazonian beef are feasible options in this direction. Disincentivizing crop production in the region, on the other hand, does not look like such a promising alternative.

As with any research paper, ours has some limitations imposed by model assumptions and the data. We discussed caveats related to technology adoption and equilibrium considerations in the last section. We also highlight that we cannot account for the value of lost biodiversity and change in rain patterns caused by deforestation, so the optimal forest gap we estimate should be seen as a lower bound. Nevertheless, we believe the numbers provided in this paper make a sensible contribution by quantifying how the current land use pattern in the Amazon is driving the region very far away from its long-run efficient forestation, and by informing the policy debate surrounding mitigation of carbon emissions from land-use change in the Amazon.

References

- Abman, R. and Lundberg, C. (2020). Does Free Trade Increase Deforestation? The Effects of Regional Trade Agreements. *Journal of the Association of Environmental and Resource Economists*, 7(1):35–72.
- Aguirregabiria, V. and Magesan, A. (2013). Euler Equations for the Estimation of Dynamic Discrete Choice Structural Models. In Choo, E. and Shum, M., editors, *Advances in Econometrics*, volume 31, pages 3–44. Emerald Group Publishing Limited.
- Aguirregabiria, V. and Mira, P. (2007). Sequential Estimation of Dynamic Discrete Games. *Econometrica*, 75(1):1–53.
- Alix-Garcia, J., Rausch, L. L., L’Roe, J., Gibbs, H. K., and Munger, J. (2018). Avoided Deforestation Linked to Environmental Registration of Properties in the Brazilian Amazon. *Conservation Letters*, 11(3):e12414.
- Alix-Garcia, J. M., Sims, K. R., and Yañez-Pagans, P. (2015). Only One Tree from Each Seed? Environmental Effectiveness and Poverty Alleviation in Mexico’s Payments for Ecosystem Services Program. *American Economic Journal: Economic Policy*, 7(4):1–40.

- Anderson, T. W. and Hsiao, C. (1981). Estimation of Dynamic Models with Error Components. *Journal of the American Statistical Association*, 76(375):598–606.
- Arellano, M. and Bond, S. (1991). Some Tests of Specification for Panel Data: Monte Carlo Evidence and an Application to Employment Equations. *Review of Economic Studies*, 58(2):277–297.
- Asher, S., Garg, T., and Novosad, P. (2020). The Ecological Impact Of Transportation Infrastructure. *Economic Journal*. ueaa013.
- Assunção, J., Gandour, C., and Rocha, R. (2017). DETERring Deforestation in the Brazilian Amazon: Environmental Monitoring and Law Enforcement. Technical report, available at <https://www.climatepolicyinitiative.org/publication/deterring-deforestation-in-the-brazilian-amazon-environmental-monitoring-and-law-enforcement/>.
- Assunção, J., Gandour, C., and Souza-Rodrigues, E. (2019a). The Forest Awakens: Amazon Regeneration and Policy Spillover. Technical report, available at <https://www.climatepolicyinitiative.org/wp-content/uploads/2020/04/TP-The-Forest-Awakens.pdf>.
- Assunção, J., McMillan, R., Murphy, J., and Souza-Rodrigues, E. (2019b). Optimal Environmental Targeting in the Amazon Rainforest. Technical report, National Bureau of Economic Research.
- Assunção, J., Gandour, C., and Rocha, R. (2015). Deforestation Slowdown in the Brazilian Amazon: Prices or Policies? *Environment and Development Economics*, 20(6):697–722.
- Assunção, J. and Rocha, R. (2019). Getting Greener by Going Black: the Effect of Blacklisting Municipalities on Amazon Deforestation. *Environment and Development Economics*, 24(2):115–137.
- Baccini, A., Goetz, S. J., Walker, W., Laporte, N. T., Sun, M., Sulla-Menashe, D., Hackler, J., Beck, P., Dubayah, R., Friedl, M., Samanta, S., and Houghton, R. A. (2012). Estimated Carbon Dioxide Emissions from Tropical Deforestation Improved by Carbon-Density Maps. *Nature Climate Change*.
- Brester, G. W. and Wohlgemant, M. K. (1993). Correcting for Measurement Error in Food Demand Estimation. *The Review of Economics and Statistics*, 75(2):352–356. Publisher: The MIT Press.

- Burgess, R., Costa, F., and Olken, B. (2019). The Brazilian Amazon's Double Reversal of Fortune. Technical report, working paper.
- Bustos, P., Caprettini, B., and Ponticelli, J. (2016). Agricultural Productivity and Structural Transformation: Evidence from Brazil. *American Economic Review*, 106(6):1320–65.
- Cai, Y. and Lontzek, T. S. (2019). The social cost of carbon with economic and climate risks. *Journal of Political Economy*, 127(6):2684–2734.
- Chimeli, A. B. and Soares, R. R. (2017). The Use of Violence in Illegal Markets: Evidence from Mahogany Trade in the Brazilian Amazon. *American Economic Journal: Applied Economics*, 9(4):30–57.
- Chomitz, K. and Gray, D. A. (1999). *Roads, Lands, Markets, and Deforestation: A Spatial Model of Land Use in Belize*. The World Bank.
- Costinot, A., Donaldson, D., and Smith, C. (2016). Evolving Comparative Advantage and the Impact of Climate Change in Agricultural Markets: Evidence from 1.7 Million Fields Around the World. *Journal of Political Economy*, 124(1):205–248.
- De Azevedo, T. R., Junior, C. C., Junior, A. B., dos Santos Cremer, M., Piatto, M., Tsai, D. S., Barreto, P., Martins, H., Sales, M., Galuchi, T., et al. (2018). SEEG Initiative Estimates of Brazilian Greenhouse Gas Emissions from 1970 to 2015. *Scientific Data*, 5:180045.
- Dominguez-Iino, T. (2021). Efficiency and Redistribution in Environmental Policy: An Equilibrium Analysis of Agricultural Supply Chains. Technical report, working paper.
- Donaldson, D. (2018). Railroads to Raj. *American Economic Review*, 108(4-5):899–934.
- Donaldson, D. and Hornbeck, R. (2016). Railroads and American Economic Growth: A “Market Access” Approach. *Quarterly Journal of Economics*, 131(2):799–858.
- EPA (2016). Social Cost of Carbon. *Environmental Protection Agency (EPA): Washington, DC, USA*.
- Ferreira, A. (2021). Satellites and fines: Using Monitoring to Target Inspections of Deforestation.
- Fezzi, C. and Bateman, I. J. (2011). Structural Agricultural Land Use Modeling for Spatial Agro-Environmental Policy Analysis. *American Journal of Agricultural Economics*, 93(4):1168–1188.

- Franklin Jr, S. L. and Pindyck, R. S. (2018). Tropical Forests, Tipping Points, and the Social Cost of Deforestation. *Ecological Economics*, 153:161–171.
- Friedlingstein, P., Jones, M., O’sullivan, M., Andrew, R., Hauck, J., Peters, G., Peters, W., Pongratz, J., Sitch, S., Le Quéré, C., et al. (2019). Global Carbon Budget. *Earth System Science Data*, 11(4):1783–1838.
- GAEZ, F. (2012). Global Agro-ecological Zones (GAEZ v3.0). *IIASA, Laxenburg, Austria and FAO, Rome, Italy*.
- Gowrisankaran, G. and Rysman, M. (2012). Dynamics of Consumer Demand for New Durable Goods. *Journal of Political Economy*, 120(6):1173–1219.
- Hansen, M. C., Potapov, P. V., Moore, R., Hancher, M., Turubanova, S., Tyukavina, A., Thau, D., Stehman, S., Goetz, S., Loveland, T., et al. (2013). High-Resolution Global Maps of 21st-Century Forest Cover Change (v1.6). *Science*, 342(6160):50–853.
- Harding, T., Herzberg, J., and Kuralbayeva, K. (2021). Commodity Prices and Robust Environmental Regulation: Evidence from Deforestation in Brazil. *Journal of Environmental Economics and Management*, 108:102452.
- Heilmayr, R., Echeverría, C., and Lambin, E. F. (2020). Impacts of Chilean Forest Subsidies on Forest Cover, Carbon and Biodiversity. *Nature Sustainability*, 3(9):701–709.
- Hendel, I. and Nevo, A. (2006). Measuring the Implications of Sales and Consumer Inventory Behavior. *Econometrica*, 74(6):1637–1673.
- Hornbeck, R. (2010). Barbed Wire: Property Rights and Agricultural Development. *Quarterly Journal of Economics*, 125(2):767–810.
- Hotz, V. J. and Miller, R. A. (1993). Conditional Choice Probabilities and the Estimation of Dynamic Models. *Review of Economic Studies*, 60(3):497–529.
- Houghton, R., Skole, D., Nobre, C. A., Hackler, J., Lawrence, K., and Chomentowski, W. H. (2000). Annual Fluxes of Carbon from Deforestation and Regrowth in the Brazilian Amazon. *Nature*, 403(6767):301–304.
- Hsiao, A. (2021). Coordination and Commitment in International Climate Action: Evidence from Palm Oil. Technical report, working paper.

IPCC (2007). *Climate Change 2007: Synthesis Report. Contribution of Working Groups I, II and III to the Fourth Assessment Report of the Intergovernmental Panel on Climate Change*. Geneva, Switzerland.

IPCC (2019). 2019 Refinement to the 2006 IPCC Guidelines for National Greenhouse Gas Inventories. Volume 4 Agriculture, Forestry and Other Land Use. Calvo Buendia, E., Tanabe, K., Kranjc, A., Baasansuren, J., Fukuda, M., Ngarize S., Osako, A., Pyrozhenko, Y., Shermanau, P. and Federici, S. (eds). *Published: IPCC, Switzerland*.

Jayachandran, S., De Laat, J., Lambin, E. F., Stanton, C. Y., Audy, R., and Thomas, N. E. (2017). Cash for Carbon: A Randomized Trial of Payments for Ecosystem Services to Reduce Deforestation. *Science*, 357(6348):267–273.

Kalouptsidi, M., Scott, P. T., and Souza-Rodrigues, E. (2021). Linear IV Regression Estimators for Structural Dynamic Discrete Choice Models. *Journal of Econometrics*, 222(1):778–804.

Lubowski, R. N., Plantinga, A. J., and Stavins, R. N. (2006). Land-use Change and Carbon Sinks: Econometric Estimation of the Carbon Sequestration Supply Function. *Journal of Environmental Economics and Management*, 51(2):135–152.

Malhi, Y., Roberts, J. T., Betts, R. A., Killeen, T. J., Li, W., and Nobre, C. A. (2008). Climate Change, Deforestation, and the Fate of the Amazon. *Science*, 319(5860):169–172.

MapBiomass, P. (2019). Collection 4.0.

Matricardi, E. A. T., Skole, D. L., Costa, O. B., Pedlowski, M. A., Samek, J. H., and Miguel, E. P. (2020). Long-term forest degradation surpasses deforestation in the Brazilian Amazon. *Science*, 369(6509):1378–1382.

Nepstad, D., McGrath, D., Stickler, C., Alencar, A., Azevedo, A., Swette, B., Bezerra, T., DiGiano, M., Shimada, J., da Motta, R. S., et al. (2014). Slowing Amazon Deforestation Through Public Policy and Interventions in Beef and Soy Supply Chains. *Science*, 344(6188):1118–1123.

Nolte, C., Agrawal, A., Silvius, K. M., and Soares-Filho, B. S. (2013). Governance Regime and Location Influence Avoided Deforestation Success of Protected Areas in the Brazilian Amazon. *Proceedings of the National Academy of Sciences*, 110(13):4956–4961.

Nordhaus, W. (2014). Estimates of the Social Cost of Carbon: Concepts and Results from the DICE-2013R Model and Alternative Approaches. *Journal of the Association of Environmental and Resource Economists*, 1(1/2):273–312.

- Pattanayak, S. K., Wunder, S., and Ferraro, P. J. (2010). Show Me the Money: Do Payments Supply Environmental Services in Developing Countries? *Review of Environmental Economics and Policy*, 4(2):254–274.
- Pellegrina, H. (2020). Trade, Productivity, and the Spatial Organization of Agriculture: Evidence from Brazil. Technical report, working paper.
- Rogelj, J., Shindell, D., Jiang, K., Fifita, S., Forster, P., Ginzburg, V., Handa, C., Kheshgi, H., Kobayashi, S., Kriegler, E., et al. (2018). Mitigation Pathways Compatible with 1.5°C in the Context of Sustainable Development. In *Global Warming of 1.5°C. An IPCC Special Report on the impacts of global warming of 1.5°C above pre-industrial levels and related global greenhouse gas emission pathways, in the context of strengthening the global response to the threat of climate change, sustainable development, and efforts to eradicate poverty*. Intergovernmental Panel on Climate Change (IPCC).
- Rosen, S., Murphy, K. M., and Scheinkman, J. A. (1994). Cattle Cycles. *Journal of Political Economy*, 102(3):468–492.
- Rust, J. (1994). Chapter 51 Structural estimation of markov decision processes. In *Handbook of Econometrics*, volume 4, pages 3081–3143. Elsevier.
- Sant'Anna, M. (2021). How Green Is Sugarcane Ethanol? *The Review of Economics and Statistics*. Forthcoming.
- Scott, P. (2018). Dynamic Discrete Choice Estimation of Agricultural Land Use. *working paper*.
- Soares-Filho, B., Moutinho, P., Nepstad, D., Anderson, A., Rodrigues, H., Garcia, R., Dietzsch, L., Merry, F., Bowman, M., Hissa, L., et al. (2010). Role of Brazilian Amazon Protected Areas in Climate Change Mitigation. *Proceedings of the National Academy of Sciences*, 107(24):10821–10826.
- Soares-Filho, B. S., Nepstad, D. C., Curran, L. M., Cerqueira, G. C., Garcia, R. A., Ramos, C. A., Voll, E., McDonald, A., Lefebvre, P., and Schlesinger, P. (2006). Modelling Conservation in the Amazon Basin. *Nature*, 440(7083):520–523.
- Souza-Rodrigues, E. (2019). Deforestation in the Amazon: A Unified Framework for Estimation and Policy Analysis. *Review of Economic Studies*, 86(6):2713–2744.
- Spracklen, D. V., Arnold, S. R., and Taylor, C. (2012). Observations of increased tropical rainfall preceded by air passage over forests. *Nature*, 489(7415):282–285.

Staver, A. C., Archibald, S., and Levin, S. A. (2011). The Global Extent and Determinants of Savanna and Forest as Alternative Biome States. *Science*, 334(6053):230–232.

Wong, P. Y., Harding, T., Kuralbayeva, K., Anderson, L. O., and Pessoa, A. M. (2019). Pay for Performance and Deforestation: Evidence from Brazil. Technical report, working paper.

Zarin, D. J., Harris, N. L., Baccini, A., Aksenov, D., Hansen, M. C., Azevedo-Ramos, C., Azevedo, T., Margono, B. A., Alencar, A. C., Gabris, C., et al. (2016). Can carbon emissions from tropical deforestation drop by 50% in 5 years? *Global change biology*, 22(4):1336–1347.

Appendix (for online publication)

- **Appendix A** presents details on the derivation of the regression equation.
- **Appendix B** describes in details how we compute the transportation costs, the conditional choice probabilities, and the counterfactual without regeneration discussed in section 7.1.
- **Appendix C** provides additional evidence of forest regeneration in our setting.
- **Appendix D** shows the supporting figures and tables.

A Regression equation derivation details

Here we provide more details on the derivation of the regression equation. The steps below follow closely in spirit the derivation in Scott (2018). From (3) and (6), we have:

$$\begin{aligned} \Phi(j, k) + r_j(w_{mt}) - \Phi(j', k) - r_{j'}(w_{mt}) - \log \left(\frac{p(j|k, w_{mt})}{p(j'|k, w_{mt})} \right) = \\ \rho E [\bar{V}(j', w_{m,t+1})|w_{mt}] - \rho E [\bar{V}(j, w_{m,t+1})|w_{mt}], \text{ for } k, j, j' \in J. \end{aligned} \quad (\text{A.1})$$

Let $\eta_j^V(w_{mt}) := \rho(E[\bar{V}(j, w_{m,t+1})|w_{mt}] - \bar{V}(j, w_{m,t+1}))$ denote the expectation error in continuation values. We can re-write (A.1) as

$$\begin{aligned} \Phi(j, k) + r_j(w_{mt}) - \Phi(j', k) - r_{j'}(w_{mt}) - \log \left(\frac{p(j|k, w_{mt})}{p(j'|k, w_{mt})} \right) = \\ \rho(\bar{V}(j', w_{m,t+1}) - \bar{V}(j, w_{m,t+1})) + \eta_{j'}^V(w_{mt}) - \eta_j^V(w_{mt}), \text{ for } k, j, j' \in J. \end{aligned} \quad (\text{A.2})$$

Another implication of the logit errors assumption is that $\bar{V}(j', w_{mt})$ has a convenient expression:

$$\bar{V}(k, w_{mt}) = \log \left(\sum_{j \in J} \exp(v(j, k, w_{mt})) \right) + \gamma, \text{ for all } k \in J, \quad (\text{A.3})$$

where γ is the Euler's gamma. From (6) and (A.3), for all $k \in J$, we can write

$$\bar{V}(k, w_{mt}) = v(l, k, w_{mt}) - \log(p(l|k, w_{mt})) + \gamma, \text{ for all } l \in J. \quad (\text{A.4})$$

We use the representation in (A.4) to cancel common continuation terms in the difference $\bar{V}(j', w_{m,t+1}) - \bar{V}(j, w_{m,t+1})$ in (A.2). Replacing (A.4) in (A.2), we have

$$\begin{aligned} \Phi(j, k) + r_j(w_{mt}) - \Phi(j', k) - r_{j'}(w_{mt}) - \log \left(\frac{p(j|k, w_{mt})}{p(j'|k, w_{mt})} \right) = \\ \rho(v(l, j', w_{m,t+1}) - v(l, j, w_{m,t+1})) - \rho \log \left(\frac{p(l|j', w_{m,t+1})}{p(l|j, w_{m,t+1})} \right) + \\ \eta_{j'}^V(w_{mt}) - \eta_j^V(w_{mt}), \text{ for } l, k, j, j' \in J. \end{aligned} \quad (\text{A.5})$$

From the definition of $v(\cdot)$, $v(l, j', w_{m,t+1}) - v(l, j, w_{m,t+1}) = \Phi(l, j') - \Phi(l, j)$. That is, all

continuation terms cancel out and we can simplify further (A.2):

$$\begin{aligned} \Phi(j, k) + r_j(w_{mt}) - \Phi(j', k) - r_{j'}(w_{mt}) - \log \left(\frac{p(j|k, w_{mt})}{p(j'|k, w_{mt})} \right) = \\ \rho(\Phi(l, j') - \Phi(l, j)) - \rho \log \left(\frac{p(l|j', w_{m,t+1})}{p(l|j, w_{m,t+1})} \right) + \\ \eta_{j'}^V(w_{mt}) - \eta_j^V(w_{mt}), \text{ for } l, k, j, j' \in J. \quad (\text{A.6}) \end{aligned}$$

Using assumption 3, for $l = j$ and $k = j'$, we can re-write (A.6) as

$$\begin{aligned} \log \left(\frac{p(j|k, w_{mt})}{p(k|k, w_{mt})} \right) - \rho \log \left(\frac{p(j|k, w_{m,t+1})}{p(j|j, w_{m,t+1})} \right) = (1 - \rho)\Phi(j, k) + \\ r_j(w_{mt}) - r_k(w_{mt}) + \eta_j^V(w_{mt}) - \eta_k^V(w_{mt}), \text{ for } j, k \in J. \quad (\text{A.7}) \end{aligned}$$

B Technical details

B.1 Transportation Costs

We build the cost of transporting agriculture products from each pixel to the nearest export port through several steps and data sources, which we detail in this section.

Data on road networks and freight costs. First, we collect georeferenced data on federal and states roads from the National Bureau of Infrastructure DNIT.³⁷ The dataset informs whether each road is paved or unpaved, as shown in Figure B.1. We convert this road network to a raster of the entire Brazilian territory that contains our 1 kilometer grid of locations and assign for each type of terrain a value that represents the cost to traverse that pixel. We allow for four different types of terrain: paved road, unpaved road, land without road, land inside protected areas without road.

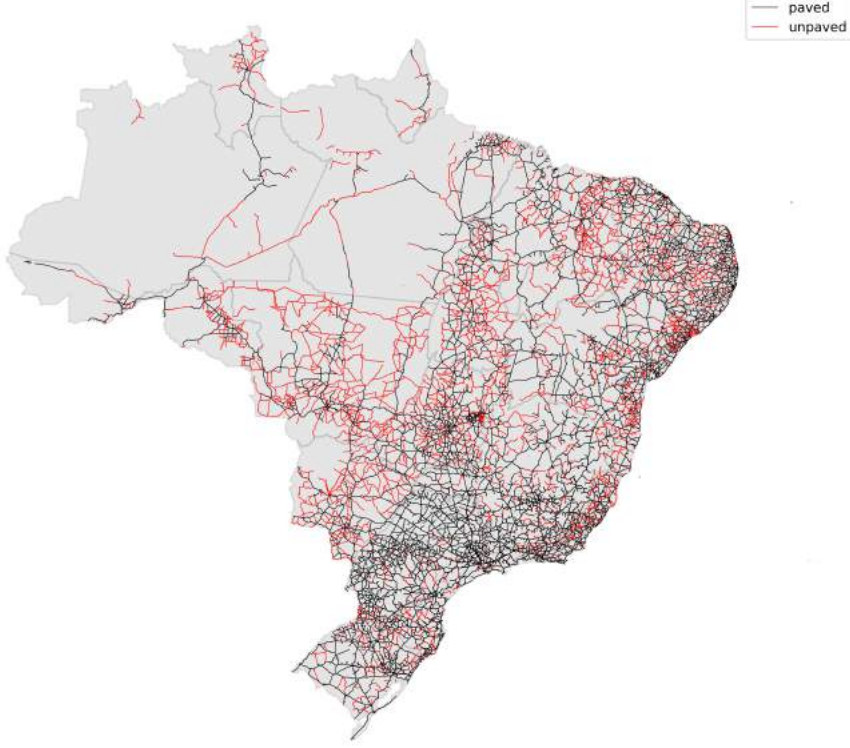
Transportation cost by land. The second step is to estimate the cost of transporting agricultural commodities on each type of pixel. We estimate this cost of traversing each type of pixel based on the internal freight costs collected by the Group of Research and Extension in Agroindustrial Logistics of the College of Agriculture Luiz de Queiroz (ESALQ). This data contains the transportation costs per ton of each product (maize and soy) between multiple municipalities for the years 2008-2013. We keep only pairs of origin/destination municipalities that connect at least one of the states of the Legal Amazon – Figure B.2 plots all origin/destination pairs we use.

We estimate the transportation cost of each type of pixel using a non-linear least squares (NLSS) as Donaldson (2018). To do so, we first set up a grid of possible values for the costs of traversing each type of road, which we denote θ . For each θ , we apply Dijkstra's shortest path algorithm to generate an estimated (non-monetary) cost of transiting products from origin m to destination n for all origin/destination pairs (m, n) in the ESALQ's data. Let $TransitCost_{m,n}(\theta)$ be the cost calculated in this process. Note that this measure has no monetary interpretation. We use ESALQ's freight cost to estimate the monetary transportation cost based on θ . For each θ , we regress the freight cost for each product and origin/destination pairs (m, n) on our non-monetary transit cost:

$$FreightCost_{m,n,c} = \beta_{0,c} + \beta_{1,c}TransitCost_{m,n}(\theta) + \epsilon_{m,n,c}, \quad (B.1)$$

³⁷Visited on 11/18/2018, <http://www.dnit.gov.br/mapas-multimodais/shapefiles>.

Figure B.1: Federal and state roads networks



This map shows the state and federal road networks we use to compute transportation costs. Black lines show paved roads and red lines show unpaved roads.

where $FreightCost_{m,n,c}$ is the monetized freight cost of transportation of one ton of product c between municipalities i and j from the ESALQ's dataset. The least squares objective function will be naturally linear in $\beta_{0,c}$ and $\beta_{1,c}$, but non-linear in θ due to the Dijkstra's algorithm. We choose the set of parameters θ that delivers the highest average R-squared.

The estimates of the best fit model is described in Table B.1. This gives us the relative costs of transporting each product by land in the whole region. This model sets the cost of traveling over pixels with paved roads equal to 1, unpaved road equal to 2, pixels with no state or federal roads equal to 5, and pixels without roads inside protected areas equal to 10. These values, especially for protected areas, seem low when compared with calibrated values from the literature (see, e.g., Souza-Rodrigues, 2019). Nonetheless, increasing the cost of travelling over pixels inside protected areas do not make much difference for the estimation because our estimated parameters are already high enough that agents avoid travelling by these pixels.

Figure B.2: Pairs of origin/destination freight costs from ESALQ



Each black line in the map represents an origin/destination pair in the ESALQ freight costs dataset.

To clarify some technical aspects, the underlying data structure to compute those costs is a graph, where each pixel is a node and possible connections between pixels are edges. To keep using the raster analogy, each pixel is connected with its 8 neighbors, provided they are inside Brazil. To visit a pixel, the agent must pay the value of that pixel. To increase the precision of our algorithm, movement in the diagonal is multiplied by $\sqrt{2}$, to account for the fact that pixels in the diagonal are farther away than the others.

Transportation cost by water. Third, we calculate the transportation cost by waterways, a commonly used transportation mode in the Amazon. Differently from roads, we cannot quantify the transportation costs between all origin/destination pairs. Instead, we model waterway transportation as an expressway to reach international markets. To do so, we collected georeferenced data on all Brazilian ports and waterways from the Ministry of Transportation. We differentiate between two types of ports: (i) final ports in which goods can be directly shipped to the international market, those with easy access to the sea; and (ii) loading ports, used as entrance to the waterways. We set the cost to traverse a pixel with waterway equal to half the cost to traverse a paved road. Figure B.3 shows the location of the main ports and the non-monetary cost to reach a final port for each loading port –

Table B.1: Estimates to monetize transportation cost

	Soybeans (1)	Maize (2)
Coefficient (β_1)	0.0723 (0.001)	0.0713 (0.001)
Constant (β_0)	5.3169 (1.341)	7.789 (1.410)
R^2	0.844	0.883
N. obs	1200	972

This table presents the estimates of the non-linear least squares regressions from equation (B.1).

final ports have zero costs.

Minimum shipping costs. In the last step, equipped with the transit costs by roads and by waterways, we compute the minimum cost to ship products from every location in our sample to the nearest final port, using Dijkstra’s algorithm. We transform this transit cost to a monetary value using the predicted values from equation (B.1). We end up with a monetary cost to transport each product from each location to an international port.

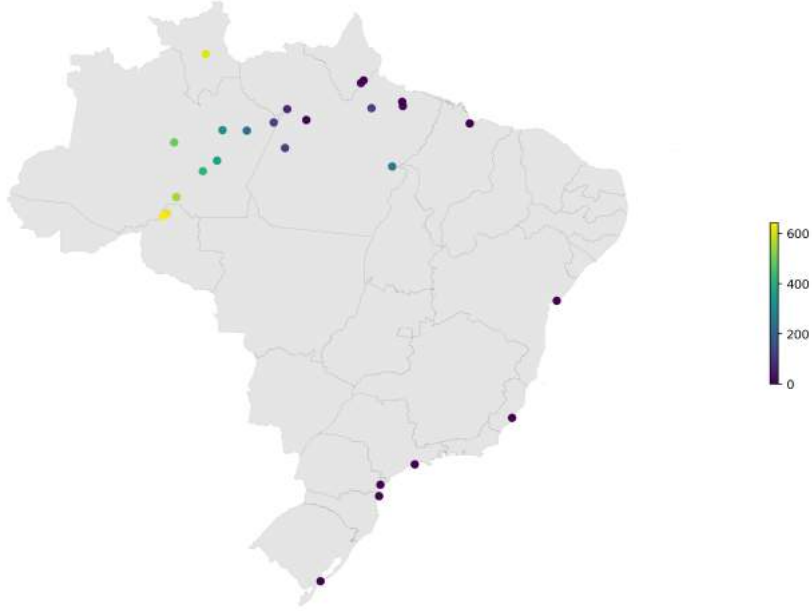
Going back to the graph data structure, a waterway node can only have an edge with another node if it is also a waterway or a port. This is how we guarantee that an agent has to go through a port to access the waterway. To keep the raster analogy, our transportation network can be seen as a three dimensional raster: one layer representing land and roads; a second layer representing waterways. Once in the waterway layer, the agent can only move on waterways. To go from the roads’ layer to the waterways’ layer the agent must access a port pixel.

B.2 Conditional Choice Probabilities

In this section we describe in more detail the computation of the conditional probabilities that make the left hand side of our main regressions. Figure B.4 shows each step of the procedure.

We start with our land use data ((a) and (b)) for two consecutive years – say 2008 and 2009. In this data we flag pixels that are out of our sample – other countries, oceans, protected areas, pixels deforested before 2000, pixels classified as urban areas or water. In step (c), for a possible transition – say forest to crop – we create a new image where we assign

Figure B.3: Ports and waterways transportation costs



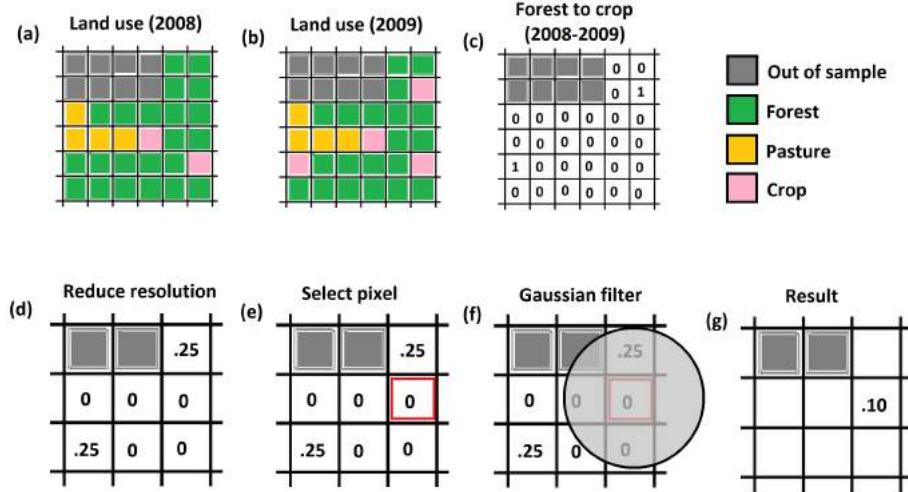
This map shows the waterways and the main ports in the Amazon we consider to estimate transportation cost. The colors in the dots show how much it costs to reach the closer final port – i.e., ports with direct access to international markets. Ports with zero cost are final ports.

1 to the pixel that made this transition and zero otherwise. Notice that we keep flagged the pixels out of our sample. In step (d), we reduce the resolution of the image – from 30 meters to 1 km in the paper, but for illustration purposes here we reduce from 4 pixels to 1 – by taking the average values. This step will still result in an image with many zeros.

In step (e) and (f), we select a pixel in our sample and apply the Gaussian filter. The Gaussian filter will take an average of the pixels around the selected pixel (flagged with a red square in (e)), assigning less weight to pixels that are farther away. These weights are determined by a Gaussian distribution with zero mean and standard deviation of 150 km. Analytically, the distribution should touch all pixels, since the Gaussian distribution has unbounded support. But, computationally the values are capped at 3 standard deviations. In this step, we exclude pixels out of our sample. In other words, we compute a normalized convolution.

In (g) we show the computed conditional probability for the selected pixel. Finally, we repeat the steps (e) and (f) for every pixel in our sample, including the non-zero ones. The result of each pixel will fill the Result image in (g). We then repeat all steps for every pair of consecutive years and every possible transition.

Figure B.4: Computing the conditional probability



This figure shows the steps we take to compute the conditional probability of land use transition. (a) and (b) show land use data, where each color corresponds to a possible use (forest, pasture, crop and out of sample); (c) illustrates the image that flags pixels that made the transition from forest to crop between 2008 and 2009 as 1. From (c) to (d) the resolution of the image is diminished by a factor of 4. The resulted image is an average of the nearby pixels, ignoring the pixels out of sample. (e) show a selected pixel for which we apply the Gaussian filter in (f). (g) shows the result of the Gaussian filter for the selected pixel.

B.3 Carbon Accounting with Forest Regeneration

As described in Section 6, to compute the counterfactual land use we begin by computing the transition matrix for each pixel. We then compute the invariant distribution of land use for each pixel. Let Table B.2 represent the transition matrix of a pixel in a given scenario. In this matrix, the value (row,column) shows the conditional probability of the pixel transitioning from land use row to land use column.

Table B.2: Transition matrix

	Forest	Crop	Pasture
Forest	ff	fc	fp
Crop	cf	cc	cp
Pasture	pf	pc	pp

This matrix represents a generic transition matrix. The value (row,column) shows the conditional probability of the pixel transitioning from land use row to land use column.

To compute the invariant distribution of each pixel in the scenario with forest regeneration we modify the above transition matrix as depicted in Table B.3. In this scenario we shut down the channel of transition from crop and pasture directly to forest. Once deforested, a pixel can only go back to being forest by going through the secondary vegetation land use.

Table B.3: Transition matrix with regeneration

	Forest	Crop	Pasture	Secondary Vegetation	
Forest	ff	fc	fp	0	
Crop	0	cc	cp	cf	
Pasture	0	pc	pp	pf	
Secondary Vegetation	(1/30)ff	fc	fp	(29/30)ff	

This matrix represents a generic transition matrix for the scenario with regeneration. The value (row,column) shows the conditional probability of the pixel transitioning from land use row to land use column.

Once in the secondary vegetation, the pixel can go back to forest with a 1/30 probability of staying as secondary vegetation. This is a simple way to capture the fact that a secondary vegetation pixel return to most of it original carbon stock after 30 years.

C Forest regeneration

In our model an agent can cease farming operations in a field, which transitions the observed land cover back to forest. This gives rise to endogenous regeneration of the forest that may challenge an established common understanding of the land dynamics in tropical forests. Here we provide evidence that this flow of land from agriculture back to forest is sizeable. We also outline possible mechanisms, some not captured directly by our model, that provides further evidence that the movement from agricultural activities to forest may reflect sound business decisions. We keep using data from the Mapbiomas project, but include two new modules of the data: forest regeneration data and pasture quality data.

The forest regeneration data classifies land use in plots previously deforested which are in transition from agricultural activities to secondary vegetation. Plots in the beginning of this transition, when vegetation is still not predominant, are classified in the ‘regeneration’ state. When plots have completed the transition and are predominantly covered by natural vegetation, they are classified as ‘secondary vegetation.’

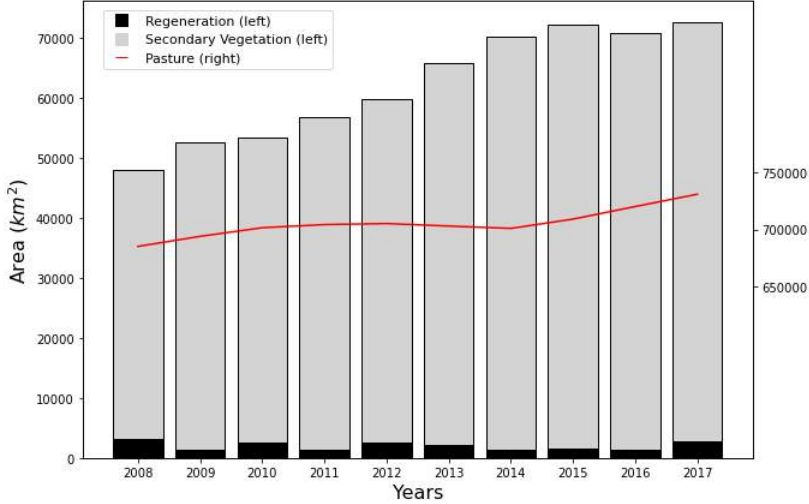
In Figure C.1 we show the total area in our sample (in squared kilometers) classified as either secondary vegetation or regeneration. Between 45,000 and 70,000 squared kilometers in our sample are secondary vegetation. To compare the magnitude, Figure C.1 plots the total area dedicated to pasture grazing. We can conclude that secondary vegetation and regeneration are indeed important types of land use in Brazilian Amazon outside of protected areas (our sample). In our model, both areas are bunched in the ‘forest’ land use.

This transition from agricultural activities back to vegetation is present in all regions of the Amazon where agricultural activities take place. Figure C.2 shows the location of secondary vegetation or regeneration. For a better visualization we down-scaled the resolution of the data, spreading the locations of secondary vegetation or regeneration in a pixel of 15km.

There are a range of possible mechanisms that help explain this movement from agriculture to secondary vegetation. Nonetheless, the research on this topic is, to the best of our knowledge, nonexistent. In our model, a farmer may decide to leave a plot fallow whenever agricultural activities become unprofitable. This could happen in practice due to a decline in soil health. Farmers may deforest a plot of land and explore it as pasture grazing in an unsustainable way, degrading the soil over time. Once the soil is severely degraded, it can become uneconomical to keep a plot as grazing area and the plot is abandoned, initiating the regeneration process.

We provide evidence in this direction by regressing an indicator variable – of whether the pixel is classified as secondary vegetation or regeneration – on dummy variables for each

Figure C.1: Regeneration and secondary vegetation



This figure depicts the total area classified as forest regeneration and secondary regeneration (left scale) in our sample over time. For comparison, we also plot total pasture area (right scale).

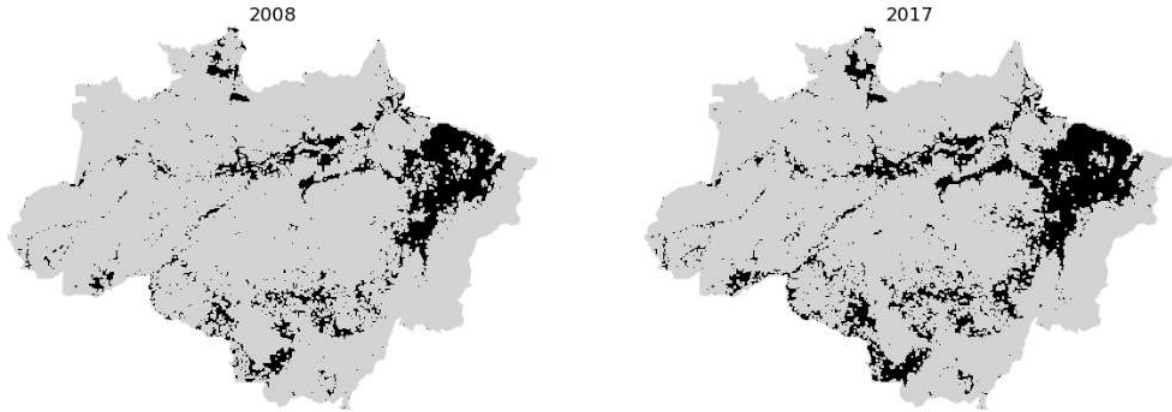
possible degradation status of pasture land in the previous year:

$$reg_{i,t+1} = \beta_0 no_deg_{i,t} + \beta_1 deg_{i,t} + \beta_2 severe_deg_{i,t} + \delta_t + X'_{i,t} \gamma + \epsilon_{i,t}, \quad (C.1)$$

where $reg_{i,t+1}$ is a dummy variable with value of 1 if pixel i in year $t + 1$ is classified as secondary vegetation or regeneration; $no_deg_{i,t}$, $deg_{i,t}$, $severe_deg_{i,t}$ denote dummy variables for pixel i that is used as pasture grazing in year t classified with no pasture degradation, pasture degradation, and severe pasture degradation respectively; $X_{i,t}$ denote controls; and δ_t is an year fixed effect. In Table C.1 we display estimates from this regression. We find that severely degraded pasture is more likely to transition to forest than pasture classified as just degraded, which in turn is more likely to transition to forest than non degraded pasture.

Besides pasture degradation, other mechanisms outside our model could explain the phenomenon of regeneration. For instance, land grabbers see deforestation as a portfolio management activity. Land grabbers may deforest multiple plots of land in hope that only some will be embargoed or caught by authorities. Those embargoed plots are abandoned while the profits from non-embargoed plots are collected. Unfortunately, investigating this mechanism requires microdata from illegal activities which are not available.

Figure C.2: Secondary vegetation map



Location of secondary vegetation. Reduced resolution to 15km for visualization purposes.

Table C.1: Regeneration and pasture degradation

	Estimate
No degradation	0.0163 (0.0002)
Degradation	0.0238 (0.0002)
Severe Degradation	0.0434 (0.0002)
Soil Suitability	Yes
Transportation cost	Yes
Year FE	Yes

This table shows the results of regressing a dummy variable indicating whether the pixel in year $t+1$ was classified as either secondary vegetation or regeneration on different pasture quality status in year t (no degradation, degradation, or severe degradation of the pasture). The omitted category is when the pixel is not being used for pasture. Controls are soil suitability for soybeans and corn, pasture suitability index, and transportation cost. We also include year fixed effects. Standard errors in parentheses are clustered at the location level.

D Appendix Figures and Tables

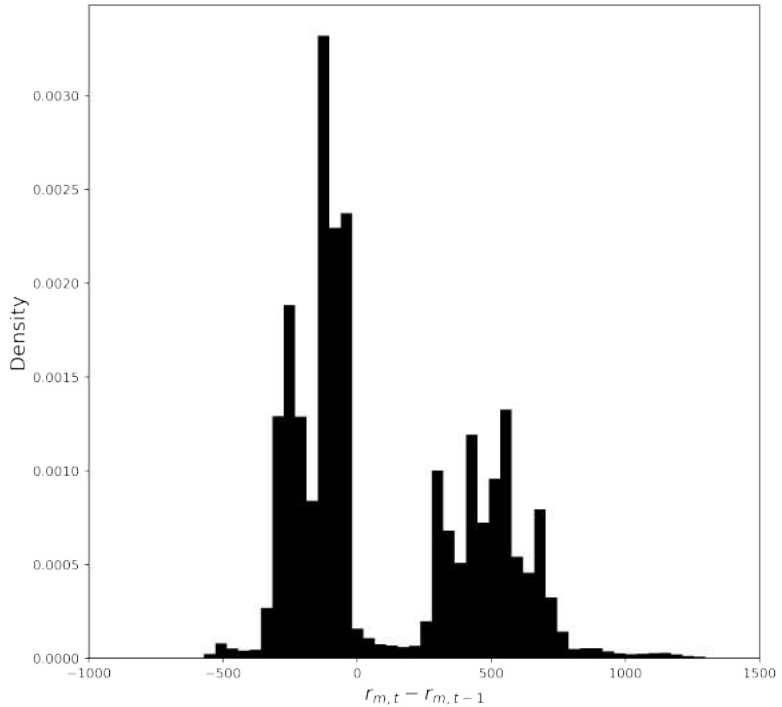


Figure D.1: This figure plots the histogram of the return in difference of the variable $(r_{m,t} - r_{m,t-1})$, showing substantial cross-sectional variation. Notice that the distribution is bimodal, since the sign of the variable depends on whether the prices of corn and soybeans increased or decreased between years. The mean value is 110.46 with a standard deviation of 347.32

Table D.1: Land Use Shares and Transitions in the Legal Amazon

Land use share		Land use transitions from 2008 (row) to 2017 (column)		
		Forest	Crop	Pasture
(1)	(2)	(3)	(4)	(5)
Forest	0.83	0.81	0.960	0.004
Crop	0.01	0.02	0.035	0.890
Pasture	0.12	0.13	0.140	0.052
				0.800

Columns (1) and (2) report land use shares for each category in 2008 and 2017, respectively. In columns (3) to (5), each cell indicates the share of fields transitioning from land use ‘row’ in 2008 to land use ‘column’ in 2017. Rows do not add up to one because we omit the ‘other’ category – i.e., non-classified pixels, urban areas, and water. This table shows the same statistics of Table 1, except that here we include pixels inside protected areas.

Table D.2: Within estimation: First stage

Regressor	Estimate (1)	Estimate (2)
$\tilde{r}_{i,t-2}$	0.04322 (0.000085)	0.04605 (1.78e-5)
$W_{j,k,i,2011}$	-0.032664 (0.000137)	-0.0478 (2.64e-5)
$W_{j,k,i,2012}$	-0.000766 (0.000298)	-0.0346 (2.63e-5)
$W_{j,k,i,2013}$	0.029048 (0.000121)	0.0538 (2.65e-5)
$W_{j,k,i,2014}$	0.017619 (0.000103)	0.0402 (2.66e-5)
$W_{j,k,i,2015}$	0.010269 (0.000074)	0.0258 (2.65e-5)
$W_{j,k,i,2016}$	-0.042952 (0.000193)	-0.0606 (2.64e-5)

This table presents the first stage estimates using the lagged values $\tilde{r}_{i,t-2}$ as an instrument for $X_{j,k,i,t}$. The first column reports regressors. For Estimate (1) standard errors in parenthesis were computed with block bootstrap with 1000 iterations in a grid of 25km by 25km. Robust standard errors in parenthesis for Estimate (2). Number of observations 79,473,168. Estimate (1) shows the results when the crop revenue net of transportation cost is a weighted average of soy and maize, where the weights are the proportion of the product in the region that the pixels lies inside. Estimate(2) shows the result when we consider that every pixel will apply a double crop system, producing soy and maize of second season in the same year. F statistics for specification (1) is 3,107,226 and for specification (2) is 3,796,531.

Table D.3: Effects of different levels of carbon tax for forestation and carbon emissions

Carbon tax (\$/ton)	Δ Forest cover (1,000km ²)	ΔCO_2 released (gigatons)
(1)	(2)	(3)
\$2.5	306 (12.7)	-15 (0.6)
\$5.0	540 (17.2)	-26 (0.8)
\$10.0	799 (19.4)	-37 (1.0)
\$20.0	977 (22.1)	-42 (1.2)

This table presents counterfactual results for the increase in forested area and decrease in emissions for different values of carbon taxes imposed on agents. Our baseline perceived carbon value implied by the model estimates is \$7.26 per ton of CO_2 . Here, we consider smaller values of carbon tax – \$2.50, \$5.00, \$10.00, and \$20.00 – added to the baseline perceived value of carbon. The column Δ Forest cover gives the difference of steady-state forest cover between the baseline scenario and the alternative scenario. The ΔCO_2 released column gives the total difference of CO_2 released between the baseline and the alternative steady state scenario for all pixels we consider in our sample. Standard errors in parenthesis were computed with block bootstrap with 1000 iterations in a grid of 25km by 25km.

Table D.4: Extensions – Crop flow profit coefficient

Regressor	Model Parameter	Estimate (2)	Estimate (3)
$X_{j,k,m,t}$	α_{crop}	0.00021 (7.91e-7)	0.00036 (1.64e-6)
$W_{j,k,m,2011}$	$\Delta\alpha_{pasture,2011}^1$	3.30e-5 (6.98e-8)	3.48045 (8.16e-8)
$W_{j,k,m,2012}$	$\Delta\alpha_{pasture,2012}^1$	-2.30e-6 (5.49e-8)	-9.31283 (4.63e-8)
$W_{j,k,m,2013}$	$\Delta\alpha_{pasture,2013}^1$	-4.00e-5 (6.28e-8)	-4.03249 (6.67e-8)
$W_{j,k,m,2014}$	$\Delta\alpha_{pasture,2014}^1$	3.00e-5 (5.97e-8)	3.23216 (5.96e-8)
$W_{j,k,m,2015}$	$\Delta\alpha_{pasture,2015}^1$	-5.65e-5 (4.58e-8)	-5.66501 (4.57e-8)
$W_{j,k,m,2016}$	$\Delta\alpha_{pasture,2016}^1$	5.59e-5 (7.18e-8)	5.78683 (9.06e-8)

This table shows the estimates of α_{crop} obtained in the second stage regression (equation 15) using Anderson and Hsiao (1981) estimator. Estimate (2) shows the result when we consider that every pixel will apply a double crop system, producing soy and maize of second season in the same year. Estimate (3) shows the result when the discount factor is set to $\rho = 0.95$ instead of $\rho = 0.9$. The first column reports regressors, while the second column displays the corresponding model parameters from Section 3.2, equations (13) and (14). Robust standard errors in parenthesis. Number of observations 79,473,168.

Table D.5: Extensions – Forest and pasture flow profits coefficients

Regressor	Model Parameter	Estimate (2)	Estimate (3)
h_m	α_{forest}	0.00073 (4.22e-7)	0.00042 (4.00e-7)
$W_{j,k,m}$	$\alpha_{pasture, 2011}^1$	7.52e-5 (3.60e-8)	5.72e-5 (3.43e-8)
$W_{j,k,m}d_m$	$\alpha_{pasture}^2$	-7.02e-7 (1.91e-9)	-7.17e-7 (1.80e-9)
Fixed effects			
	$\Phi(pasture, forest)$	-0.623 (1.58e-4)	-0.30 (0.0001)
	$\Phi(crop, forest)$	-0.968 (3.01e-4)	-0.42 (0.0002)
	$\Phi(crop, pasture)$	-0.597 (3.11e-4)	-0.281 (0.0002)
	$\Phi(pasture, crop)$	-0.200 (3.07e-4)	-0.11 (0.0002)
	$\bar{\alpha}_{pasture}$	0.157 (1.84e-4)	0.04 (0.0001)
	$\bar{\alpha}_{crop}$	-0.650 (2.55e-4)	-0.75 (0.0002)

This table presents the OLS estimates of equation (9), using $\hat{\alpha}_{crop}$ and $\Delta\alpha_{pasture,t}^1$ estimated in equation (15) using Anderson and Hsiao (1981). Estimate (2) shows the result when we consider that every pixel will apply a double crop system, producing soy and maize of second season in the same year. Estimate (3) shows the result when the discount factor is set to $\rho = 0.95$ instead of $\rho = 0.9$. The first column reports regressors, while the second column displays the corresponding model parameters from Section 3.2, equations (13) and (14). Robust standard errors in parenthesis. Number of observations 79,473,168.

Table D.6: Extensions – Efficient forestation and counterfactual carbon tax

Carbon tax	Δ Forest cover ($1,000km^2$)	ΔCO_2 released (billion tons)
(1)	(2)	(3)
Panel A. Double cropping agriculture		
\$2.5	161	-8
\$5.0	304	-15
\$10.0	521	-25
\$20.0	750	-34
\$33.7	874	-37
Panel B. Discount rate ($\rho = 0.95$)		
\$2.5	346	-18
\$5.0	638	-32
\$10.0	954	-46
\$20.0	1156	-52
\$44.28	1264	-54

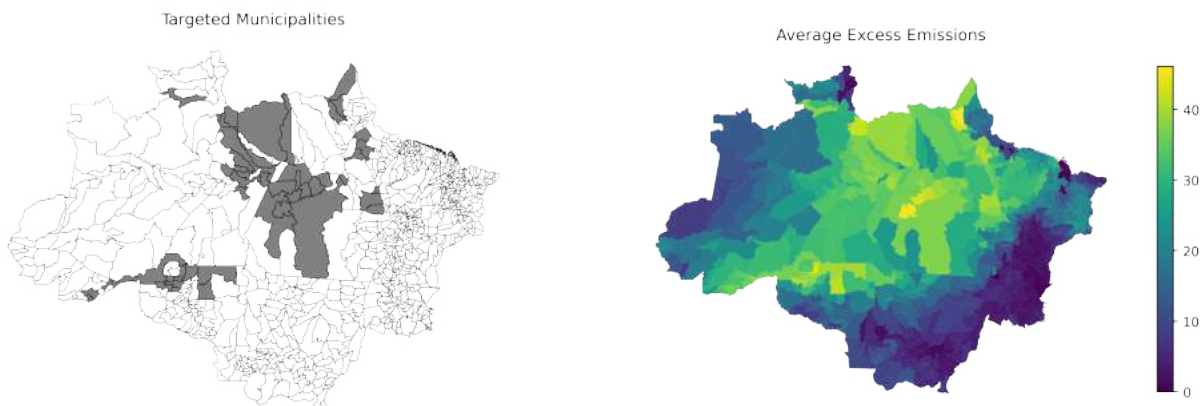
This table presents counterfactual results for the increase in forested area and decrease in emissions for different values of carbon taxes imposed on agents for two model extensions. Panel A shows the result when we consider that every pixel will apply a double crop system, producing soy and maize of second season in the same year. Our baseline perceived carbon value implied by the model estimates is \$16.29 per ton of CO_2 . Here, we consider smaller values of carbon tax – \$2.50, \$5.00, \$10.00, \$20.00, and \$33.70 – added to the baseline perceived value of carbon. The last row shows the result for the efficient scenario, where the total perceived value of carbon is of \$50. Panel B shows the results derived using a discount factor of $\rho = 0.95$ instead of $\rho = 0.9$. Our baseline perceived carbon value implied by the model estimates is \$5.72 per ton of CO_2 . The column Δ Forest cover gives the difference of steady-state forest cover between the baseline scenario and the alternative scenario. The ΔCO_2 released column gives total the difference of CO_2 steady-state released between the baseline and the alternative scenario for all pixels we consider in our sample.

Table D.7: Extensions – Carbon accounting with forest regeneration

Carbon tax (US\$/ton)	Carbon price (US\$/ton)	Share of forest < 30 yrs	ΔCO_2 released (billlion tons)
(1)	(2)	(3)	(4)
0 [†]	7.26	0.51	
2.50	9.76	0.43	-13.35
5.00	12.26	0.35	-25.85
10.00	17.26	0.24	-42.42
20.00	27.26	0.14	-55.45
42.73 [‡]	49.99	0.07	-62.41

This table presents results for avoided emissions from different carbon taxes for an alternative scenario in which secondary vegetation (forest recently converted from pasture and crops) stays 30 years with zero carbon stock, realizing its full potential after 30 years. Column (3) presents out of the total forest area in the long run, the share which is secondary vegetation (age < 30 years). First row ([†]) displays the status quo scenario and the last row ([‡]) the efficient forestation scenario.

Figure D.2: Targeted municipalities and average excess emissions



These maps show: the location of the 52 targeted municipalities in our counterfactual exercise (left); the excess emissions in municipalities measured in thousand tons of CO_2 per km^2 (right).

Table D.8: Average excess emissions by municipalities

Municipality	State	CO2	Municipality	State	CO2
Serra do Navio	AP	46.12	Tucuruí	PA	38.17
Trairão	PA	45.70	Iracema	RR	38.15
Rurópolis	PA	43.70	Itupiranga	PA	38.07
Cujubim	RO	43.65	Ariquemes	RO	37.98
Pedra Branca do Amapari	AP	43.00	Oiapoque	AP	37.89
São João da Baliza	RR	42.29	Medicilândia	PA	37.83
Caroebe	RR	42.28	Parintins	AM	37.75
Placas	PA	41.88	Vitória do Xingu	PA	37.48
Rondolândia	MT	41.46	Altamira	PA	37.46
Breves	PA	40.88	Boa Vista do Ramos	AM	37.34
Buritis	RO	40.87	Urucará	AM	37.01
Monte Negro	RO	40.37	Itaituba	PA	36.60
Barreirinha	AM	39.95	Rio Preto da Eva	AM	36.59
Novo Repartimento	PA	39.87	Santarém	PA	36.47
Colniza	MT	39.65	Cacaúlândia	RO	36.36
São Luiz	RR	39.55	Óbidos	PA	36.35
Rio Crespo	RO	39.24	Nhamundá	AM	36.32
Machadinho D'Oeste	RO	39.21	Melgaço	PA	36.25
Uruará	PA	39.15	Porto Velho	RO	36.25
Acrelândia	AC	39.01	Itapiranga	AM	36.19
Silves	AM	38.90	Xapuri	AC	36.13
Oriximiná	PA	38.86	Aveiro	PA	36.11
Belterra	PA	38.50	Epitaciolândia	AC	36.11
Alto Paraíso	RO	38.26	Senador Guiomard	AC	36.09
Afuá	PA	38.20	Nova Olinda do Norte	AM	36.05
São Sebastião do Uatumã	AM	38.18	Itacoatiara	AM	35.89

This table shows 52 municipalities from the highest to lowest excess emissions measured in thousand tons of CO2 per km^2 .